11-1959

Annual summary research report in metallurgy for July 1958–June 1959

Ames Laboratory

Annual summary research report in metallurgy for July 1958–June 1959

Abstract
This report is prepared from material submitted by the group leaders of the Laboratory.

Disciplines
Metallurgy

IS-17

ANNUAL SUMMARY
RESEARCH REPORT IN METALLURGY
for
July 1958 - June 1959
by
Ames Laboratory Staff

AMES LABORATORY
RESEARCH AND DEVELOPMENT REPORT
U.S.A.E.C.

UNCLASSIFIED

IS-17

Metallurgy and Ceramics(UC-25)
TID 4500, August 1, 1959

UNITED STATES ATOMIC ENERGY COMMISSION

Research and Development Report

ANNUAL SUMMARY
RESEARCH REPORT IN METALLURGY

for

July 1958 - June 1959

by

Ames Laboratory Staff

November 1959

Ames Laboratory
at
Iowa State University of Science and Technology
F. H. Spedding, Director
Contract W-7405 eng 82

UNCLASSIFIED

This report is distributed according to the category Metallurgy and Ceramics (UC-25) as listed in TID-4500, August 1, 1959.

Printed in USA. Price $ 2.75 . Available from the

Office of Technical Services
U. S. Department of Commerce
Washington 25, D. C.

CONTENTS

METALLURGY

APPENDIX

ANNUAL SUMMARY RESEARCH REPORT IN METALLURGY

For the Period July 1958 - June 1959

This report is prepared from material

submitted by the group leaders

of the Laboratory

Previous research reports in this series are:

ISC-35	ISC-323
ISC-41	ISC-339
ISC-56	ISC-396
ISC-69	ISC-423
ISC-74	ISC-453
ISC-76	ISC-485
ISC-79	ISC-506
ISC-113	ISC-531
ISC-130	ISC-575
ISC-133	ISC-607
ISC-137	ISC-644
ISC-171	ISC-708
ISC-193	ISC-759
ISC-220	ISC-835
ISC-248	ISC-903
ISC-290	ISC-977
ISC-300	ISC-1050

METALLURGY

(Annual Report, July 1958 - June 1959)

Under the direction of F. H. Spedding, H. A. Wilhelm,
O. N. Carlson, P. Chiotti, W. L. Larsen,
R. E. McCarley, D. T. Peterson and
J. F. Smith

1. Separation Studies

1.1 Liquid-Liquid Extraction (H. A. Wilhelm and M. L. Andrews)

The work on liquid-liquid extraction as a means for purifying inorganic materials of interest in pure metal preparation has continued. Barium and strontium separation studies employing a system consisting mainly of barium and strontium chlorides, thiocyanate, water and tributyl phosphate have resulted in setting up conditions for effective separation of these two elements.

Earlier work had shown the tributyl phosphate to give promising separation and transfer of strontium to the organic phase when certain amounts of thiocyanate were present. Studies of a number of variables have given conditions for increased separation and transfer. The use of NaSCN in place of NH_4SCN improved both the separation and transfer. Additions of NaCl seemed to increase the separation with essentially no effect on total transfer. The amount of total (both Sr and Ba) transfer to the organic phase is cut down markedly by the addition of HCl or NaAc.

HAc, NaOH and NH_4OH decrease the transfer only slightly. As expected, increasing the Ba and Sr concentration from 0.5M to 0.67M as well as increasing the volume of organic relative to the aqueous phase increased the amount of total transfer to the organic phase. Keeping other variables constant, the amount of total transfer increased sharply with the thiocyanate up to a concentration equal to the total Ba + Sr equivalent concentration. Diminishing additional transfer was observed for higher thiocyanate concentrations.

A number of countercurrent extraction experiments have been performed on this system and the Ba and Sr analytical data for the products from a 20 stage extractor were determined in terms of X-ray fluorescence intensities only. The exact ratios of Ba to Sr will be determined later from a calibration curve that is being prepared.

Conditions and results of extraction experiments being performed with a 20 stage extractor are exemplified by one experiment as follows:

Feed solution - 2.0M NaSCN, 0.67M $BaCl_2$, 0.67M $SrCl_2$
20 ml. of this aqueous solution was introduced at stage 11 on each cycle.

Scrub solution- 5 M NaCl (aqueous)
10 ml. introduced at stage 1 per cycle

Organic - Tri-n-butyl phosphate 30 ml. per cycle at stage 20.

Analytical data after 140 cycles of operation indicated as X-ray fluorescent intensity ratios (where 50-50 weight mixture of Ba and Sr

sulfates gave a Ba to Sr intensity ratio of about 0.09) are, (a) Aqueous phase delivered at stage 20 intensity ratio = 0.55, (b) the Ba to Sr intensity ratio was too low to obtain a numerical value in the organic (strontium rich) solution delivered at stage 1. The numerical value at stage 7 was only 0.002. Although actual analytical results are not yet available, it is obvious that considerable separation is effected and that the strontium rich product is delivered from the extractor in the organic phase while the barium rich product follows the aqueous phase.

Experiments are under way to determine not only the variation in Ba to Sr ratio but also the behavior of the other ions in the extractor during operation at steady state.

1.2 Pyrometallurgical Separations

1.2.1 Distribution of Pa^{233} Between Mg-38 w/o Th and Uranium-Rich Solutions (P. Chiotti and P. F. Woerner)

Uranium can be separated from a thorium-uranium alloy by dissolution of the thorium in magnesium. The uranium separates as a finely divided solid or liquid phase (99+% U) depending on the temperature. If enough chromium is added to form U-5.2 w/o Cr eutectic the uranium can be separated as a liquid U-5.2 w/o Cr phase on heating to above the U-Cr eutectic temperature, 860°C. In the case of neutron irradiated thorium containing U^{233} as well as its 27.4 day half-life precursor Pa^{233} the course of the protactinium in such a separation is of considerable importance.

Some results on the distribution of protactinium between Mg-38 w/o Th and uranium as well as U-5.2 w/o Cr were presented in a previous report, ISC-1050. Further experiments have been conducted. The experimental procedure was the same as that described previously, ISC-1050, except that the components were more vigorously agitated at the equilibration temperatures to assure attainment of equilibrium and in some samples both the 90 kev and 300 kev gamma transitions characteristic for Pa^{233} were counted.

Previous results have shown that the Pa^{233} is essentially quantitatively extracted into the uranium phase. Consequently after equilibration the protactinium activity in the magnesium-rich phase was relatively low. Calculations indicated that an appreciable part of this residual 90 kev activity might be due to Th^{234} a 24 day half-life daughter product (UX_1) of uranium which exhibits a 92 kev gamma transition.

To check this possibility unirradiated Mg-38 w/o Th alloy was equilibrated with uranium or U-5.2 w/o Cr using the same source materials and procedures employed in previous experiments. As expected the major part of the Th^{234} activity moved into the magnesium solution. The distribution coefficients, counts/min/gm in the uranium phase divided by the counts/min/gm in the magnesium phase, for the uranium and U-5.2 Cr equilibrations were 0.10 and 0.045 respectively. The thorium contents of the uranium phase and the U-5.2 Cr phase on equilibration with Mg-38 Th as determined in past work are roughly 1.0 and 0.5 w/o. On this basis the calculated distribution coefficients

expected are 0.085 and 0.035 respectively and are in reasonably good agreement with the measured values. On the basis of these data it was possible to correct the 90 kev measurements on the magnesium-rich phase for the other equilibrations. The final results obtained are presented in Table I. All the residual 90 kev activities in the Mg-38 w/o Th phase were corrected for the contribution of Th^{234} except for the first equilibration entered in the Table. In this case the initial 90 kev activity in the Mg-Th alloy employed was relatively low and the final activity was of the same order as the calculated correction term. In all other cases the correction term was of the order of 5 to 15% of the residual activity. The values for the distribution coefficient and decontamination factor show considerable scatter. However, since over 99% of the protactinium was extracted into the uranium phase, in each case small errors in measuring the final activity in the magnesium phase would be expected to produce a large variation in these values. It may be concluded from these data, that protactinium would essentially quantitatively follow the uranium phase in the separation of uranium from irradiated thorium by extraction with magnesium.

1.2.2 Pyrometallurgical Purification of Uranium, (P. Chiotti and S. J. S. Parry)

Work has continued on the separation of minor constituents from uranium by selective oxidation or reduction reactions utilizing liquid zinc and KCl-LiCl eutectic as solvents, $ZnCl_2$ as oxidizing agent and magnesium or calcium as reducing agents.

Table I

Distribution of Pa^{233} Between Mg-38 w/o Th and Uranium or U-5.2 w/o Cr Phases

Charge gms	Phase	Counting Level kev	Activity 10^4c/m/g	Distr.[1] Coeff.	D.F.[2]	% Pa^{233} Extracted From Mg Phase
26.5	Mg-38Th	90	0.280[3]	91	357	99.7
95.4	U	"	25.4			
33.1	Mg-38Th	"	0.485	74	206	99.5
90.8	U	"	35.8			
33.1	Mg-38Th	300	0.42	46	238	99.6
90.8	U	"	19.3			
62.0	Mg-38Th	90	3.57	72	132	99.2
101.5	U-5.2Cr	"	256			
66.6	Mg-38Th	"	3.68	159	271	99.6
96.5	U-5.2Cr	"	586			
33.2	Mg-38Th	300	0.241	193	415	99.8
86.7	U-5.2Cr	"	46.5			

1. Distribution coefficient, counts per minute per gram (c/m/g) in the uranium phase divided by c/m/g in magnesium-rich phase.
2. Decontamination factor, initial c/m/g divided by final c/m/g in magnesium-rich phase.
3. Uncorrected value.

The first step in the process involves the dissolution of uranium containing various amounts of impurities in either liquid zinc or KCl-LiCl-$ZnCl_2$ fused salt. Some exploratory data on the rate of dissolution of massive uranium in this salt mixture at temperatures up to 650°C were given in a previous report. Further work has shown that the reaction becomes very vigorous at 700°C. The reaction of uranium with zinc is also vigorous at this temperature. Although quantitative data have not been obtained at 700°C, qualitative observations indicate that a salt solution or zinc alloy containing 10 to 15 w/o uranium can be obtained without particular difficulty. Air must be excluded from the reaction otherwise uranium precipitates as the oxide.

Tantalum has proved to be a satisfactory container for this reaction. Some exploratory tests indicate that a high silicon steel may also be satisfactory.

If one considers the first step to be the dissolution of impure uranium in KCl-LiCl eutectic containing 10 to 20 w/o $ZnCl_2$, the uranium as well as the more active impurities will be oxidized by the $ZnCl_2$ and move into the salt phase. The impurities more noble than zinc will collect in the metallic zinc produced. From available free energy data it may be expected that metals such as nickel, iron, niobium, molybdenum and many others would remain quantitatively in the zinc phase. The liquid zinc phase containing these impurities can be readily separated and discarded or the zinc purified by distillation and reused. The uranium in the salt phase can be recovered by equilibration with a zinc-magnesium alloy.

In principle it should be possible by controlling the amount of magnesium to reduce the uranium and leave components more active than uranium in the salt phase. The uranium can be recovered by distilling away the zinc and magnesium. The same principles apply if uranium is first dissolved in zinc and then equilibrated with an inert fused salt such as KCl-LiCl to which is added controlled amounts of $ZnCl_2$. The more active components compete for the available chlorine introduced by the $ZnCl_2$. Consequently, the step wise removal of the more active components may be feasible. Finally, the addition of an excess of $ZnCl_2$ will move the uranium into the salt phase leaving the more noble impurities in the zinc phase. The uranium can be removed from the salt by reduction with a zinc-magnesium alloy. Such a separation procedure should be very effective in separating uranium from all elements except those of similar thermodynamic and chemical properties. Metals of particular interest which may fall into this latter category are Cr, Zr, Th, Pa, Pu and the rare-earth elements.

Free energy of formation data for the metal chlorides are available. However, since neither the salt solutions nor the zinc solutions considered are ideal, it is not possible to predict from these data alone what degree of separation can be accomplished by simple equilibration procedures. Knowledge of the solubility and activity coefficients of the various components in the salt and zinc phases would be particularly helpful. Uranium, zirconium and thorium are known to

exhibit a large negative deviation from ideality in zinc-rich solutions; presumably the other metals of interest such as protactinium and the rare-earth metals do likewise. Little is known concerning the activity of the chlorides of these metals in KCl-LiCl eutectic. The data that is available indicate that these halides may also show a large negative deviation in the salt phase, probably due to complex ion formation.

It is the purpose of the present investigation to determine experimentally the degree of separation of impurities from uranium which can be achieved by selective oxidation-reduction reactions in the system KCl-LiCl/zinc. Some solubility and thermodynamic data pertinent to this investigation are available and are discussed below.

The elements Fe, Cr, Zr, U, and Th all form compounds with zinc which are only slightly soluble in zinc at 500°C. At 700°C the solubility of U or Th is still less than one a/o while the solubilities of Zr, Fe, and Cr are in the range of 3 to 5 a/o. Consequently the reaction of uranium with liquid zinc at 500 to 700°C results in a two phase alloy consisting of solid U_2Zn_{17} and a dilute zinc liquid. An alloy containing 10 w/o uranium will be in the form of a slurry with about 30 w/o solid U_2Zn_{17}. The presence of appreciable amounts of Fe, Cr, Zr, or Th as impurities will also result in the formation of their respective zinc compounds or possibly ternary or more complex solid phases. Plutonium, cerium and presumably other rare earth metals and

protactinium also form stable compounds with zinc, which are only sparingly soluble in liquid zinc in the temperature range of 500 to 700°C. The standard free energies of formation for the binary zinc compounds of U, Th, and Zr have been determined. These data along with the free energy data for the chlorides are helpful in estimating the equilibrium distribution of these elements between fused KCl-LiCl and liquid zinc. Some of these data pertinent to this investigation are given in Table II. The data for the chlorides of Zr, Pu, and Pa were taken from Glassner's compilation, Report ANL-5750, and the data for the other chlorides were taken from W. J. Hamer, et al., J. Electrochem. Soc. 103 No. 2, 8-16 (1956). The free energy data on the intermetallic compounds in Table II and the solubility data given in Table III were taken from data presented in previous reports of this series and the present report.

Since the zinc solutions in equilibrium with the intermetallic compounds are very dilute, it may be concluded that the partial molar free energy of solution of the solid solute in zinc is of the same order as the standard free energy of formation of the compound. In the case of thorium the solubility in zinc at 500°C is 0.0061 a/o or $N = 6.1 \times 10^{-5}$. Assuming the partial molar free energy of solution of zinc to be negligible, we can write for the partial molar free energy of thorium relative to pure solid thorium,

$$\overline{\Delta F} = -43,000 = RT \ln \gamma \cdot 6.1 \times 10^{-5}.$$

Solving for the activity coefficient we obtain a value of the order of 10^{-8} which indicates a very strong negative deviation from Raoult's Law.

Table II

Standard Free Energy of Formation of Some Chlorides and Intermetallic Zinc Compounds

Compound	-ΔF° K cal/mole 500°C	600°C	700°C
$CrCl_2$	71	68	65
$ZnCl_2$	74	72	70
$ZrCl_3$	167	162	157
$ZrCl_2$	118	115	112
$ThCl_4$	228	221	215
UCl_3	172	168	163
$MgCl_2$	124	120	117
$PuCl_3$	189	184	179
$PaCl_3$	202	197	192
$CeCl_3$	219	214	209
Th_2Zn_{17}	86	80	74
U_2Zn_{17}	54	46	38
$ZrZn_{14}$	34	--	--
$ZrZn_6$	31	27	22

Table III

Solubility of Th, U, and Zr in Zinc

Component	Temp. °C	N	w/o	Activity Coeff. Relative to Pure Solid Component
U	500	9.0×10^{-5}	0.033	2.5×10^{-4}
"	600	76.0 "	0.27	2.3×10^{-3}
"	700	410.0 "	1.48	1.3×10^{-2}
Th	500	6.1×10^{-5}	0.022	1.2×10^{-8}
"	600	53.0 "	0.19	1.8×10^{-7}
"	700	280.0 "	0.99	1.9×10^{-6}
Zr	500	5.0×10^{-3}	0.70	4.9×10^{-8}
"	600	14.0 "	1.96	1.2×10^{-5}
"	700	31.0 "	4.28	3.7×10^{-4}

Consequently in the selective reduction of $ThCl_4$ or the chlorides of the rare earths, U, Zr, Pa or Pu the strong interaction of these metals with zinc will play an important part in determining the extent to which reaction takes place.

In a system consisting of a solution of zinc containing uranium and other components and KCl-LiCl eutectic the more active metallic components compete for the available chlorine on the addition of $ZnCl_2$. Considering the reactions

$$Th_2Zn_{17} + 4ZnCl_2 \rightarrow 2ThCl_4 + 21Zn$$

$$U_2Zn_{17} + 3ZnCl_2 \rightarrow 2UCl_3 + 20Zn$$

$$2ZrZn_{14} + 3ZnCl_2 \rightarrow 2ZrCl_3 + 31Zn$$

The data in Table II show that $\Delta F°$ for these reactions are sufficiently large and negative (-54 to -78 K cal.) so that Th, Zr, and U should move quantitatively into the salt phase in the presence of excess $ZnCl_2$. However, in the case of zirconium there is some question whether it is present in the salt phase as trivalent or divalent zirconium in the temperature range of 500 to 700°C. If it is present in the divalent state the reaction is less favorable. Furthermore, the uncertainty in the free energies of formation of the zirconium chlorides is rather large. Metals whose chlorides have an appreciably lower free energy of formation than that of $ZnCl_2$ such as Mo, Fe and Ru would be expected to remain quantitatively in the zinc phase. In the case of chromium the free energy of the chloride is about the same as that for zinc, and the extent to which it remains in the zinc phase will depend primarily on its interaction with zinc.

1.2.3 Distribution of Various Components Between KCl-LiCl Eutectic Containing Excess $ZnCl_2$ and Zinc (P. Chiotti and S. J. S. Parry)

A. Distribution of Mo, Zr, Cr and U

The distributions of Mo, Zr, Cr and U between the salt and zinc-rich phases have been measured. The results and some experimental conditions are summarized in Table IV. The charge in each case was

Table IV

Distribution of U, Mo, Cr, and Zr in the Phases Resulting from the Equilibration of U-5w/o M alloy, Zinc and KCl-LiCl-$ZnCl_2$ Salt Mixture

Charge gms	Equilibration Temp. °C	Mixing Time hrs.	Chemical Analyses Phase	%U	%M
U-Mo*-2.1 Zn 19.0 Salt**-21.3	650	0.5	Metal Salt	0.033 7.62	0.21 Mo <2 ppm Mo
U-Mo- 2.1 Zn -19.4 Salt- 21.4	650	1	Metal Salt	0.051 7.51	0.28 Mo <2 ppm Mo
U-Mo- 1.4 Zn-20.5 Salt- 21.6	650	1.5	Metal Salt	0.059 5.43	0.12 Mo <2 ppm Mo
U-Mo- 3.0 Zn- 19.8 Salt- 31.0	625	20***	Metal Salt	0.57 7.30	0.57 Mo <2 ppm Mo
U-Cr- 2.3 Zn- 19.7 Salt- 17.0	650	0.5	Metal Salt	0.09 10.45	0.23 Cr 0.04 Cr
U-Cr- 2.1 Zn- 19.4 Salt- 18.8	650	1	Metal Salt	0.07 8.72	0.18 Cr 0.04 Cr
U-Cr- 2.3 Zn- 21.9 Salt- 18.7	650	1.5	Metal Salt	0.14 9.68	0.21 Cr 0.04 Cr
U-Cr- 1.9 Zn- 19.7 Salt- 29.6	625	20***	Metal Salt	0.08 5.07	0.19 Cr 0.07 Cr
U-Zr- 2.15 Zn- 20.5 Salt- 22.6	650	1.0	Metal Salt	0.02 7.34	0.014 Zr 0.35 Zr
U-Zr- 1.8 Zn- 20.5 Salt- 22.6	650	1.5	Metal Salt	0.01 6.13	0.011 Zr 0.26 Zr

Table IV con'd.

* Uranium-rich alloy prepared by arc-melting. Alloy constituent nominally 5 w/o.

** The initial composition of the salt was 80 w/o KCl-LiCl eutectic and 20 w/o $ZnCl_2$.

*** In all other experiments listed the components were mixed at temperature in a rocking furnace which oscillated through an arc of approximately 180° sixty times per minute. In these two experiments the furnace oscillated only two times per minute.

sealed in a welded tantalum container which was protected from atmospheric oxidation by a graphite liner and an external steel casing. The tantalum container was charged and sealed under an atmosphere of inert gas. The charge was mixed at temperature in a rocking furnace which oscillated through an arc of approximately 180° sixty times per minute. The rate of oscillation in two of the experiments, as noted in the table, was only two cycles per minute. With the more rapid rate of oscillation, equilibrium is apparently attained in a half hour or less; this is not generally true for the slower, two cycle per minute rate. After equilibration the charge was permitted to settle for one hour and then furnace cooled to room temperature.

It is apparent from the data that molybdenum, and to a lesser extent, chromium, remain in the zinc phase. No molybdenum could be detected in the salt phase with a test sensitive to as low as 2 ppm. The average distribution coefficient for chromium, % Cr in Zn/% Cr in salt, for the four equilibrations is 5.1. Uranium and to

a lesser extent zirconium concentrated in the salt phase. The average distribution coefficient for uranium, % in salt/% in Zn is 195. The average distribution coefficient for zirconium in the two zirconium equilibrations is 24. Further work is being carried out in an attempt to determine these distribution coefficients more precisely.

Similar experiments have been conducted with U-5 w/o Nb and U-5 w/o Fe arc-melted alloys. Chemical analyses show that both iron and niobium concentrate in the zinc phase as expected but the actual amount remaining in the salt phase is uncertain. These experiments will be repeated.

B. Distribution of Protactinium-233

Similar experiments with uranium containing trace amounts of Pa^{233} show that in the presence of excess $ZnCl_2$ the protactinium moves into the salt phase. Samples of uranium or U-5.2 w/o Cr containing protactinium were prepared by equilibration with neutron irradiated Mg-38 w/o Th alloy. Consequently these samples contained 0.5 to 1.0 w/o thorium. Samples cut from the uranium obtained from these equilibrations were sealed in tantalum crucibles, along with zinc and KCl-LiCl-20 w/o $ZnCl_2$ and equilibrated at 700°C and furnace cooled. The distribution of protactinium was determined by radiochemical analyses. The results obtained are summarized in Table V.

Table V

Distribution of Pa^{233} Between Zinc Solution and $KCl-LiCl-ZnCl_2$ Fused Salt

Typical charge gms.	Pa^{233}, 300 kev Activity, 10^4 c/m/g	Distribution Coeff. $\frac{c/m/g\ salt}{c/m/g\ zinc}$
U[a] - - - 1.95		
Salt[b] - 18.6	12.8	230[c]
Zinc - 31.0	0.056	
U[a]-5.2 w/o Cr - 1.4		
Salt - - - - - - 20.0	13.4	145[d]
Zinc - - - - - 29.5	0.075	

a. Uranium containing trace amounts of Pa^{233}

b. Initial composition of salt was 80 w/o KCl-LiCl eutectic and 20 w/o $ZnCl_2$

c. Average value for four different equilibrations

d. " " " eight " "

1.2.4 Reduction of Protactinium from the Salt Phase with Magnesium or Calcium (P. Chiotti and S. J. S. Parry)

To study the effectiveness of a zinc-rich magnesium or calcium alloy in reducing protactinium from the salt phase, samples were equilibrated at 700°C with a zinc phase containing 2 to 4 w/o calcium or magnesium or both. Mixing of the charge was continued at 500°C for a half hour. It was then permitted to settle for a half hour and rapidly cooled with an air blast. Fifteen equilibrations were carried out using magnesium or calcium or both as the reducing agent. Calcium was used in some of the experiments, since it is a more effective reductant than magnesium for oxides that might be formed due to the inadvertant contamination of the charge with oxygen. The charge composition and experimental results for four typical equilibrations are given in Table VI. The protactinium recovered in these experiments and eleven other similar experiments ranged from 69 to 96%. A thin black film was observed at the metal-salt interface. Radiochemical analyses of this film showed some concentration of protactinium on the film but not enough to account for the low yields. Some loss to other interfaces must have occurred.

It may be concluded from the results obtained that zinc containing 2.0 to 4.0 w/o of either magnesium or calcium will effectively reduce protactinium from the salt phase. No significant advantage of calcium over magnesium as the reducing agent was indicated by the results.

Table VI

Distribution of Pa^{233} Between KCl-LiCl Rich Salt and Zn-rich Alloy Containing 2.0 to 4.0 w/o of Magnesium or Calcium

Initial Charge gms.		Pa^{233}, 300 Kev Activity, 10^4 c/m/g		Distribution Coeff. c/m/g zinc / c/m/g salt	Calculated Residual Reductant in Zinc Phase
		Zinc	Salt		
U[a]	1.50	50	0.211	237	3.3 w/o Mg
Zn	10.67				
Mg	0.62				
Salt[b]	10.00				
U-Cr	1.27	124	0.112	1108	2.5 w/o Mg
Zn	11.02				
Mg	0.58				
Salt	10.00				
U-Cr	1.10	122	0.034	3590	3.18 w/o Ca
Zn	8.53				
Ca	0.80				
Salt	10.00				
U-Cr	1.95	140	0.028	5000	3.5 w/o Mg
Zn-7w/o Mg	19.15				
Salt	17.15				

a. Uranium containing trace amounts of protactinium.

b. The initial composition of the salt was 80 w/o KCl-LiCl eutectic and 20 w/o $ZnCl_2$.

1.2.5 Distribution of Components on the Addition of Controlled Amounts of Oxidizing or Reducing Agent (P. Chiotti and S. J. S. Parry)

In all the foregoing experiments an excess of oxidizing agent, $ZnCl_2$, or an excess of reducing agent, magnesium or calcium was employed. Thermodynamic data indicate that a more selective separation of the components may be attained by the addition of controlled amounts of oxidizing or reducing agent. For example, on the addition of a small amount of $ZnCl_2$ to a system consisting of KCl-LiCl salt and zinc containing 10 to 15 w/o impure uranium, the more active components will compete for the available chlorine. In the case of U, Th and Zr the reactions of interest are the following:

1. $4/3\ U_2Zn_{17} + 2ThCl_4 \rightarrow 8/3\ UCl_3 + Th_2Zn_{17} + 17/3\ Zn$

   $\Delta F°$, 500, 600, 700°C = -17, -25, -28 K cal. respectively

2. $U_2Zn_{17} + 11Zn + 2ZrCl_3 \rightarrow 2UCl_3 + 2ZrZn_{14}$

   $\Delta F°$, 500, 600, 700°C = -26, -24, -18 K cal. respectively

3. $Th_2Zn_{17} + 61/3\ Zn + 8/3\ ZrCl_3 \rightarrow 2ThCl_4 + 8/3\ ZrZn_{14}$

   $\Delta F°$, 500, 600, 700°C = -18, -7.3, +4.0 K cal. respectively.

The compound $ZrZn_{14}$ is not stable above 545 °C; it decomposes peritectically to give $ZrZn_6$ and zinc at this temperature. Therefore the values given for $\Delta F°$ for reactions 2 and 3 are for the formation of the corresponding number of moles of $ZrZn_6$ on the right side of the equations at temperatures above 500°C. The $\Delta F°$ values for these reactions indicate that uranium would move into the salt phase ahead

of either thorium or zirconium. Small scale experiments in which controlled amounts of anhydrous $ZnCl_2$ were added to the charge showed that the sequence in which these metals moved into the salt phase was uranium, thorium and zirconium. This sequence was followed at 500°C and at 700°C. The reverse order was observed on reduction with zinc-magnesium alloy. In each case considerable overlap in the movement of the uranium, thorium and zirconium was observed. Experiments and equipment are being designed to investigate these reactions on a larger scale. Several kilograms of zinc and salt phases will be employed. Consequently, quantitative data will be presented at a later date.

1.2.6 Precipitation of Solutes as Hydrides from Liquid-Metal Solvents (P. Chiotti and P. F. Woerner)

Some of the metallic elements form relatively stable hydrides with distinct crystal structures and rather well defined stoichiometry. The possibility of precipitating such elements from liquid-metal solvents by contacting the solutions with hydrogen at one atmosphere pressure is being investigated. Suitable solvents must, of course, be metals which do not react appreciably with hydrogen, and since the stability of hydrides in general decreases rapidly with an increase in temperature the solvents must be relatively low melting. The elements of Groups II B, III B, and Mg, Al, Sn, Pb and Bi or eutectic mixtures of these would not be expected to react appreciably with hydrogen at one atomosphere pressure, and might serve as suitable solvents.

Assuming the formation of a solid hydride MH_2 in equilibrium with the saturated solvent then the following relations apply:

$$M(s) + H_2(g)\ 1\ atm. \longrightarrow MH_2(s) \quad \Delta F = \Delta F^\circ$$

$$(M, soln) \longrightarrow M(s) \quad \Delta F = -\overline{\Delta F} = -RT \ln a_M$$

$$(M, soln) + H_2(g)\ 1\ atm \rightleftharpoons MH_2(s) \quad \Delta F = O$$

We can therefore write,

$$\Delta F^\circ = RT \ln a_M = RT \ln N_M + RT \ln \gamma_M.$$

Where a_M and γ_M are respectively the activity and activity coefficient of M in solution relative to pure solid M at the temperature in question. It may be seen that, other things being equal, the larger the negative value for the standard free energy of formation, ΔF°, the more complete the precipitation will be. For a given ΔF° value the precipitation reaction is less favorable the smaller the value for the activity coefficient. Consequently, solutes which interact strongly with the solvent, those which show a large negative deviation from Raoult's Law are less likely to be precipitated.

A review of the available data on the metal hydrides, shows that the alkali, alkaline earth, Group III A, Group IV A, the lanthanide and actinide metals form rather well defined crystalline hydrides. The standard free energy of formation as a function of the atomic number indicates maxima between the Group II A and IV A metals and maxima at the beginning of the lanthanide and actinide series. These hydrides also show the highest thermal stability, that is, the temperature is also relatively high at which the hydrogen dissociation pressure is one atmosphere. It is apparent that these are the hydrides of the more electropositive metals.

Since a strong interaction between solute and solvent is undesirable as explained above, a solvent with about the same electronegativity value as the solutes to be precipitated would be desirable. From this point of view magnesium should be the most suitable solvent of those considered above.

The precipitation of calcium, yttrium, cerium and thorium from magnesium in contact with hydrogen at one atmosphere pressure has been investigated. Experimental procedure and the results on the precipitation of ThH_2 have been given in detail in Report ISC-928, "Precipitation of Thorium as Thorium Hydride from Thorium-Magnesium Solutions", by Paul F. Woerner and P. Chiotti, August 1957. The results for thorium are reproduced in Table VII for comparison with the

Table VII

Residual Solute Content in Liquid Magnesium Equilibrated with Hydrogen at One Atmosphere Pressure

	Temperature °C				
Solute	625	650	700	800	900
Ca w/o	6.9	7.3	8.9	12.1	15.3
" N x 10^2	---	4.6	5.5	7.6	9.7
Y w/o	---	0.11	0.32	2.04	8.90
" N x 10^2	---	0.029	0.088	0.565	2.61
Ce w/o	---	>13.0	---	---	---
" N x 10^2	---	>2.51	---	---	---
Th w/o	---	6.00	10.3	24.6	43.4
"N x 10^2	---	0.66	1.20	3.30	7.40

results obtained for calcium, yttrium and cerium. In the case of cerium the initial alloy contained 13 w/o cerium and no precipitation of the hydride was observed in the range 900 to 625°C. The precipitation of yttrium hydride is the most effective of the four solutes. The data obtained for the residual yttrium content in the temperature range covered, 653-918°C, can be expressed by the relation,

$$\log N_Y = -\frac{8,452}{T} + 5.634.$$

Yttrium can also be precipitated from a solution of Mg-55 w/o Zn. In this case the residual yttrium content of the solvent in the temperature range 485 to 844°C can be represented by the relation

$$\log N_Y = -\frac{4,865}{T} + 3.208.$$

At near the freezing point of the solvent, 340°C, $N_Y = 1.87 \times 10^{-5}$ and at 900°C, $N_Y = 0.115$. Comparing these results with those obtained for yttrium in a magnesium solvent, (Table VII), it is seen that at any given temperature the residual yttrium content is greater in the Mg-55 w/o Zn solvent. However, the latter solvent remains liquid to a much lower temperature, about 340°C as compared to 650°C for magnesium, and the final residual yttrium in solution is lower.

Although quantitative analyses have not been completed, it appears that the precipitation of thorium from the same solvent is almost completely suppressed by the presence of zinc. This is not surprising in view of the strong interaction between thorium and zinc as indicated by the relatively

high free energy of formation of thorium-zinc compounds given elsewhere in this report.

2. Preparation of Pure Compounds

2.1 Preparation of Pure Vanadium Pentoxide (R. E. McCarley and J. W. Roddy)

Work on the preparation of high purity vanadium pentoxide, as one phase of a program for the preparation of high purity vanadium compounds, has been completed during this period. The final procedure used for the purification was that given in the semi-annual report ending June 30, 1958 (ISC-1050). Further work was directed mainly towards the verification and elucidation of some of the experimental results given in the last report.

The over-all chlorine efficiency at a temperature of 450°C was again determined for the reaction,

$$2V_2O_5 + 3C + 6Cl_2 = 4VOCl_3 + 3CO_2,$$

using the rotating glass reactor previously described. The resulting value of 88% chlorine conversion at a flow rate of 1.90 liters/min. agreed well with the value 90% found previously. Moreover, the conversion of vanadium to $VOCl_3$ was consistent in all cases, i.e., about 75% of the total vanadium present in the oxide used.

Additional chlorination reactions were performed as an effort to determine the variation of charge temperature as a function of chlorine flow rate. In general, the charge temperature was found to be ca 75° greater than the furnace temperature at 350°, but only 15° higher at 450°. These values varied somewhat with flow rate; the very fast and very slow rates resulted in a decrease of the charge temperature.

Analytical data for V_2O_5 produced by the hydrolysis of $VOCl_3$ in aqueous ammonia and subsequent ignition of the precipitated NH_4VO_3 is given in Table VIII. The hydrolysis was effected in solutions both with and without added citric and tartaric acids, which act as masking agents for impurity elements. From this data it may be concluded that even the V_2O_5 obtained from the hydrolysis of undistilled $VOCl_3$ in the absence of the complexing agents is of a high order of purity. Addition of the complexing agents, however, was effective in the further reduction of the silicon content in the product.

The data given in Table IX indicate the effectiveness of the distillation step with respect to removal of impurities from the $VOCl_3$. A sample of $VOCl_3$ as obtained from the chlorination reaction was fractionated through a small column packed with glass helices. As the distillation progressed samples of the distillate were collected at regular intervals and were hydrolyzed with aqueous ammonia. The resulting precipitates of NH_4VO_3 were ignited and their impurity content determined by spectrographic analysis. These results showed that within the limits of the analytical method only silicon, titanium and copper were reduced by the distillation step. Since silicon may be removed just as effectively by addition of citrate or tartrate ions to the hydrolysis solution, the distillation becomes desirable only when the silicon content must be maintained below ca. 25 ppm. With inclusion of the distillation step it seems probable that V_2O_5 of 99.99 percent purity can be produced consistently by this process.

2.2 Preparation of Yttrium Fluoride (F. A. Schmidt, O. N. Carlson and F. H. Spedding)

The large scale preparation of yttrium fluoride was continued through the middle of September, 1958. At that time enough yttrium fluoride was on

TABLE VIII

Analytical Data for V_2O_5 Resulting from Hydrolysis of of $VOCl_3$ and Subsequent Ignition of NH_4VO_3

Sample No.	History of $VOCl_3$	Complexing Agent		Spectrographic Analysis[a] (Ppm)						
		Name	Conc. Ppm	Si	Mg	Cr	Cu	Ti	Ca	Fe
1	not distilled	---	---	129	<20	<20	<20	<20	<20	ND[b]
2	not distilled	citrate	1000	25	<20	<20	<20	<20	<20	~30[c]
3	pot residue after distillation	---	---	71	<20	<20	<20	<20	<20	ND
4	pot residue after distillation	citrate	1000	25	<20	<20	<20	<20	<20	~30[c]
5	distilled	citrate	1000	<20	<20	<20	<20	<20	<20	~30[c]
6	distilled	---	---	24	<20	<20	<20	<20	<20	ND
7	distilled	tartrate	1000	<20	<20	<20	<20	<20	<20	ND

a Elements not listed were below the limits of spectrographic detection

b The symbol ND means the element was not determined

c Determination of iron by a colorimetric procedure gave ca. 11 ppm.

Table IX

Analytical Data for V_2O_5 Obtained from the Fractional Distillation of $VOCl_3$

	Spectrographic Analysis (in ppm)						
Sample No.	Si	Fe	Mg	Cr	Cu	Ti	Ca
1[a]	105	<100	<20	<20	50	40	30
2	150	<100	<20	<20	30	~13	<20
3	50	<100	<20	<20	27	~16	<20
4	35	<100	<20	<20	25	20	<20
5	35	<100	<20	<20	22	22	<20
6	30	<100	<20	<20	25	24	<20
7	33	<100	<20	<20	20	25	<20
8	38	<100	<20	<20	22	20	<20
9	33	<100	<20	<20	24	~17	<20
10	35	<100	<20	<20	25	20	<20
11	35	<100	<20	<20	23	~16	<20
12	35	<100	<20	<20	22	~14	<20
13[b]	78	<100	<20	<20	50	43	35

[a] Sample before distillation.

[b] Sample from residue after distillation.

hand to meet the anticipated demands for the next few months and the large scale production schedule was interrupted.

The amounts of yttrium fluoride produced and shipped to Corwith Co., Chicago, Illinois during the period of this report are given in Table X.

Table X

Production of YF_3 During Last Half of 1959

Month	Oxide Used	Fluoride Produced	Fluoride Shipped
July	4,800.0 lbs.	6,105.0 lbs.	6,086.5 lbs.
Aug.	4,356.1 lbs.	5,535.0 lbs.	3,047.4 lbs.
Sept.	1.550.0 lbs.	1,957.3 lbs.	4,063.5 lbs.
Oct.	---	---	3,014.2 lbs.
Nov.	---	---	2,288.0 lbs.
Dec.	---	---	2,081.5 lbs.

A small amount of yttrium fluoride of low oxygen content was prepared by vacuum distillation. Production grade yttrium fluoride was placed in a graphite crucible together with a small amount of platinum. The fluoride was then vacuum distilled at 1700°C and collected on an air cooled condenser. The fluoride condensate contained 180 ppm oxygen.

Because of the economic value of the YF_3 used in the salt extraction refining process (see Section 3.4.4) the recovery of the yttrium salt was studied. It was found that the $CaCl_2$ can readily be separated from the YF_3

by water leaching. The insoluble YF_3 containing small amounts of CaF_2 are then dried in air and given a high temperature hydrofluorination treatment. The fluoride recovered in this way is equivalent to or slightly lower in oxygen content than that obtained by the direct hydrofluorination of Y_2O_3. The reclaimed fluoride has been used successfully both as an extractant and as a starting material for metal preparation.

More complete details on the preparation of YF_3 are given in a report recently published by the staff of this laboratory. The report entitled "Studies of the Preparation, Properties and Analysis of High Purity Yttrium Oxide and Yttrium Metal at the Ames Laboratory" by C. V. Banks, O. N. Carlson, A. H. Daane, V. A. Fassel, R. W. Fisher, E. Olson, J. Powell and F. H. Spedding, is a U. S. Atomic Energy Commission Report, IS-1, July 1959.

3. Metal Preparation and Purification Studies

3.1 Vanadium

3.1.1 Purification by Iodide Process (O. N. Carlson and C. V. Owen)

A large, all-vycor reaction vessel was constructed for use in vanadium crystal bar experiments. Earlier work using a small vycor unit indicated that higher metal yields were obtained than with the inconel unit. This was also realized in the larger vycor unit. Good quality bars of vanadium weighing approximately one half pound were consistently produced in this vycor unit. This retort produced 50% more metal in the same length of time than the inconel retort. This increased efficiency was

believed to be due to the ability of the system to withstand high temperature heating throughout. However, the difficulties in sealing the quartz system each time offset most of the advantages of the higher growth rate.

Analytical methods for determining the metallic impurities were worked out by the spectroscopic group during this period. The results of these analyses showed that the metallic contamination in the final metal, in particular iron and chromium, was much greater than had been estimated previously, often running well over 1000 ppm of each. This contamination obviously came from the inconel retort since metal prepared in the vycor unit was low in these impurities. Two approaches were taken to minimize this contamination. The first was to find a different metal from which to build the reaction vessels. Since no nickel pickup was reported from the inconel unit, commercially pure nickel was used to construct a retort. The results were very unsatisfactory. The nickel was not extremely pure so that contamination from iron, chromium, and copper remained at a high level in the vanadium. Furthermore, the nickel would not withstand air oxidation at the furnace temperature of 800°C resulting in failure of the retort. Monel metal was also tried but the metallic impurities remained high in the resulting vanadium, and it lacked the oxidation resistance required for the high operating furnace temperatures.

The second approach to lowering the metallic contamination was to modify the existing inconel retort. This was accomplished by protecting the inner inconel wall, as nearly as possible, with a liner of molybdenum. This inner liner acted as a vapor barrier and minimized the migration of

gaseous iodine to the inconel walls and back to the hot wire. This modification resulted in a marked reduction in the amount of Cr and Fe present in the vanadium to amounts of less than 200 ppm of each.

Growth experiments to establish the proper feed temperature and filament temperature were performed and most of the metal produced during this period was produced using these conditions. A feed material temperature between 800-825°C and a filament temperature of either 1000°C or 1300°C were found to represent optimum conditions. Bars grown at 1300°C were somewhat larger and heavier but were less dense than those grown at 1000°C.

The feed material employed in most of this work was millings obtained from massive bomb reduced vanadium. An investigation of methods for producing a cheaper and more easily processed feed material was undertaken. Vanadium sponge prepared by the reduction of V_2O_5 with carbon at 1550°C was tried as the feed material. This sponge did not work too well, however, probably because of a film on the surface of the sponge which inhibited iodine attack. The vanadium obtained with this material was very high in oxygen content. Further heating of the sponge for 12 hours under vacuum at 1550°C produced a better grade of metal with a bright, metallic surface. When the latter was used as feed material the growth rate and purity were equivalent to metal made using bomb reduced vanadium as the feed material.

The development of a spectroscopic method of analyzing for metallic impurities and the acquisition of a vacuum fusion apparatus for analyzing the oxygen and hydrogen content of the metal, has given a more quantitative

picture of the actual purity of vanadium metal produced by thermal decomposition. Vanadium produced in the modified inconel and vycor retorts has a silicon content of 50-100 ppm and a maximum of all other metallic impurities, including Fe and Cr, of approximately 400 ppm. The contents of the common interstitial impurities in a typical batch of vanadium were as follows: 200 ppm C, 100 ppm O, 24 ppm N and 10 ppm H.

Attempts are now being made to purify the metal further by zone refining techniques. A new zone melter was recently purchased from the Ecco corporation.

An electrolytic polishing and etching technique was developed for use on vanadium metal and excellent microstructures have been obtained. The electrolyte is composed of nine parts of ethyl alcohol to one part hydrochloric acid. A two to five minute cyclic polish and etch in this electrolyte consistently produces a smooth surface and clearly reveals the grain boundaries and other features of the microstructure.

3.2 Niobium (columbium)

3.2.1 By Carbon Reduction of Nb_2O_5 - (H. A. Wilhelm and E. R. Stevens)

Work was continued on the reduction of Nb_2O_5 by carbon with small additions of TiO_2 to the charge. It appears from work on this problem that small amounts of TiO_2 added to certain charges of Nb_2O_5 and carbon are beneficial for the production of ductile niobium.

In studying the effects of TiO_2 additions to the reduction charge, an exploration of the reaction between TiO_2 and carbon was also made. The

results indicate that the reaction between carbon and TiO_2 in a vacuum at elevated temperature evolves CO gas and gives TiC and/or TiO. Several series of reactions were of concern for these studies. They involved charges corresponding to 2 to 8 mols of carbon per 2 mols of TiO_2. These reactions were carried out in the same environment as the reduction of Nb_2O_5 by carbon. The amount of TiC and/or TiO resulting from the reaction depended on the amount of carbon used. Experiments also indicated that the amount of the oxide-carbide product seemed quite dependent of the final temperature at which the reaction was investigated on the holding time at this temperature. It is believed that TiO is volatile under the conditions in which the reactions were investigated i.e., high vacuum and a temperature in the vicinity of 2000°C.

Earlier work on the reduction of Nb_2O_5 by carbon was accomplished by running each reduction charge individually. Consequently, each reduction was held at temperatures for varying lengths of times, and the final holding temperatures varied somewhat with each experiment. However, the series reductions which have been done recently have been carried out in groups, each series being treated simultaneously in a large graphite heater with a 16-inch induction coil. This was done to eliminate the heretofore varying conditions. A typical series which was investigated was charged accordingly:

$$Nb_2O_5 + (5 + z)C + (y)TiO_2$$

$z = 0, +.1, +.2, +.3, -.1, -.2, -.3$

with $y = +.1$ in each.

The data indicated that when the ratio, z/y had a value within the range -0.5 to +2.0, "good metal" was obtained from the reduction. "Good metal" refers to that metal (Nb) which cold-rolled satisfactorily from an arc-melted button of the reduction product. It should be pointed out that although the z/y ratio between the limits of -0.5 to +2.0 apparently gave "good metal" in the series cited, a general relationship has not been established.

Other data have indicated that the final temperature of the reduction and the holding time at this temperature may be important for the elimination of titanium and oxygen in the form of a volatile lower oxide of titanium.

Work will continue on this problem during the next period.

3.2.2 Purification of Niobium Metal by the Iodide Process

(R. E. McCarley and W. Tadlock)

Investigation of the purification of niobium metal by the iodide process has continued with extension of feed metal temperatures to 800°C. The apparatus and procedures were essentially the same as those described in the previous report of this series (ISC-1050) except that for temperatures above 550°C a vycor vessel was used.

Analytical data for the purified metal indicate that the percentage removal of both carbon and nitrogen remains nearly constant regardless of the feed metal temperature. In a majority of the experiments a reduction of ca 90% in carbon content and ca 80% in nitrogen content was observed. A major departure from this trend was observed only in a few isolated cases.

The results of this work have shown that little purification with respect to oxygen can be attained by this process. Over the entire temperature range at which the feed metal was maintained, i.e., 300 to 800°C, the transfer of oxygen to the crystal bar metal was rapid. In many cases the oxygen content in the crystal bar was found to be greater than that in the feed metal, although the oxygen content in the feed metal had not increased significantly during the growth of the crystal bar. These results indicate that some surface oxidation of the feed metal occurred during the sealing of the vycor vessel, even though this operation was performed with a rapid stream of argon passing through the vessel. The oxide coating was then transferred quantitatively to the crystal bar during its growth. Further work on this process will be directed towards a solution of the oxygen transfer problem.

Data on the growth rate of the filament as a function of feed metal temperature also has been obtained in the course of this work. Figure 1 shows the growth of the filament as a function of time for various feed temperatures and a constant filament temperature of 1250 $\pm$ 30°C. The growth rates in $ohm^{-1}min^{-1}$ as obtained from the curves in Fig. 1 are given in Fig. 2 as a function of the feed metal temperature.

Interpretation of the behavior illustrated in Fig. 2 is difficult owing to an insufficient knowledge of the properties of niobium iodides. However, the presence of the two maxima in the growth rate-feed temperature curve indicates that a different set of reactions is responsible for the niobium

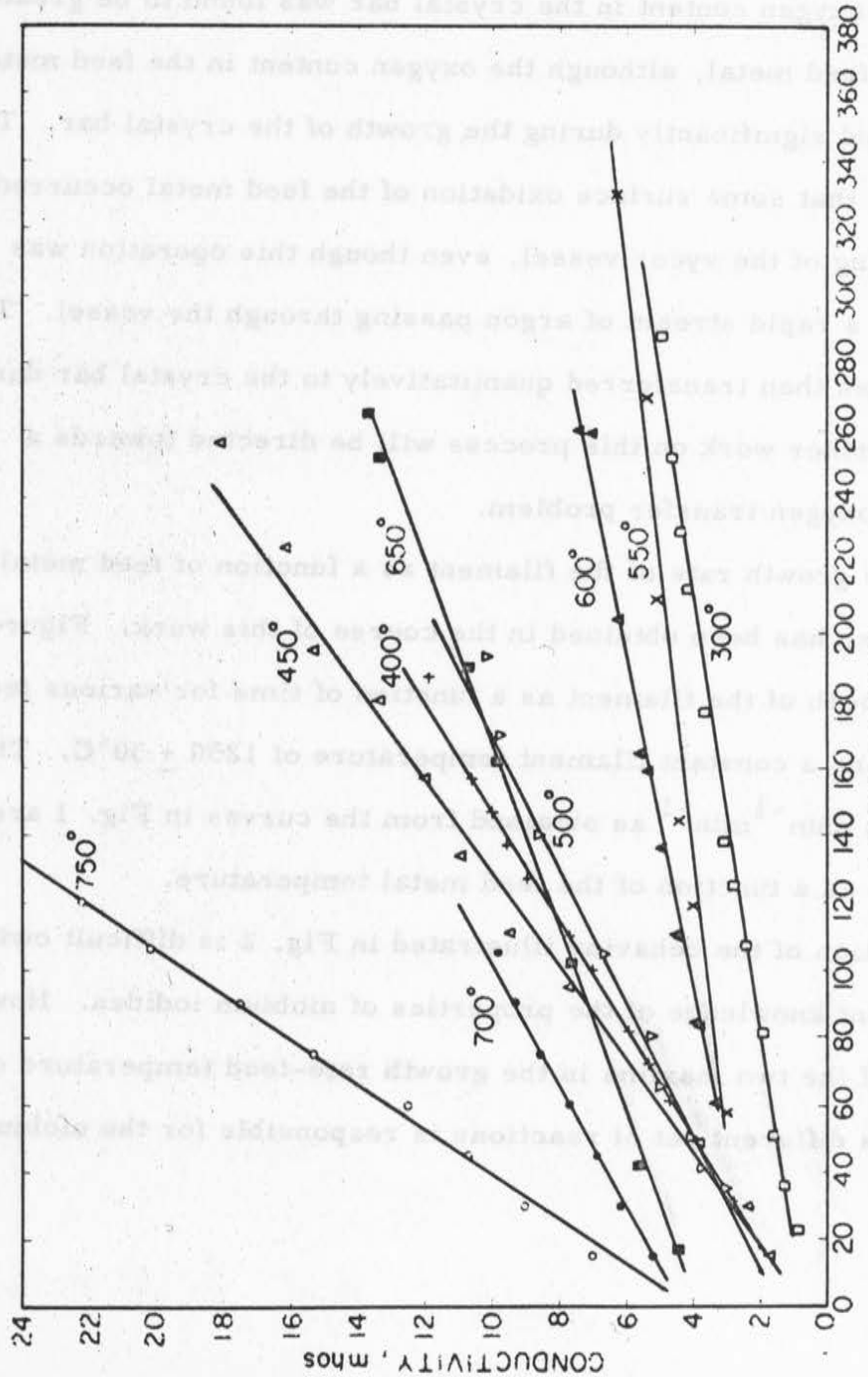

Fig. 1. Filament growth vs. time at the feed temperatures shown and the filament temperature 1250 ± 30°C.

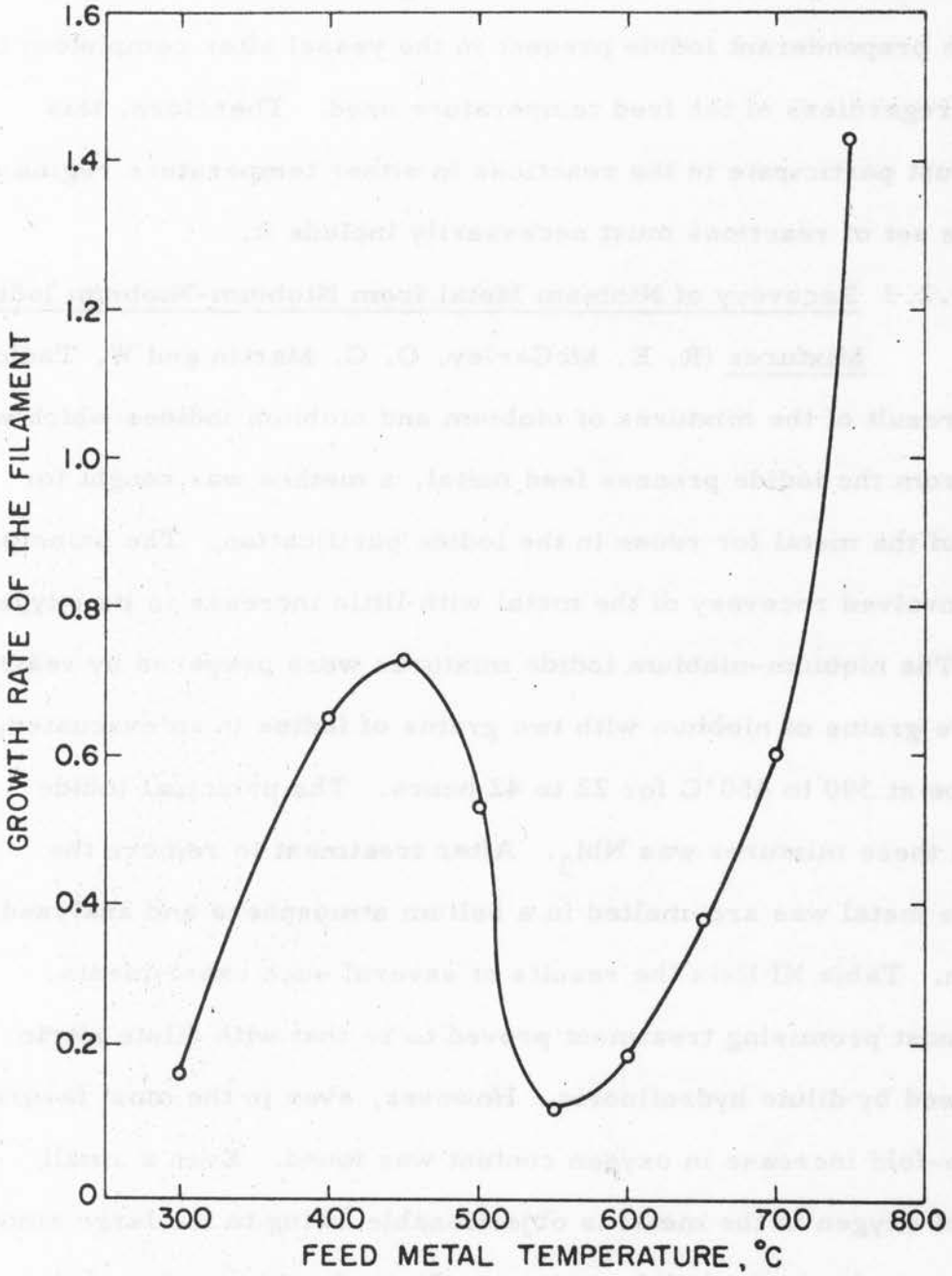

Fig. 2. Rate of filament growth vs. feed temperature at the filament temperature 1250 ± 30°C.

transport in the high and low temperature regions. It has been found that NbI_3 is the preponderant iodide present in the vessel after completion of a reaction, regardless of the feed temperature used. Therefore, this species must participate in the reactions in either temperature region and a plausible set of reactions must necessarily include it.

3.2.3 Recovery of Niobium Metal from Niobium-Niobium Iodide Mixtures (R. E. McCarley, O. C. Martin and W. Tadlock)

As a result of the mixtures of niobium and niobium iodides which were obtained from the iodide process feed metal, a method was sought for recovery of the metal for reuse in the iodide purification. The principal problem involved recovery of the metal with little increase in its oxygen content. The niobium-niobium iodide mixtures were prepared by reacting twenty-five grams of niobium with two grams of iodine in an evacuated, sealed tube at 390 to 450°C for 22 to 42 hours. The principal iodide present in these mixtures was NbI_3. After treatment to remove the iodides the metal was arc-melted in a helium atmosphere and analyzed for oxygen. Table XI lists the results of several such experiments.

The most promising treatment proved to be that with dilute nitric acid followed by dilute hydrofluoric. However, even in the most favorable case a two-fold increase in oxygen content was found. Even a small increase of oxygen in the metal is objectionable owing to the large amount of oxygen transfer in the iodide process. Since the acquisition of the vycor vessel it has been found more convenient to sublime the iodides out of the feed metal at 800°C following the completion of a run. This

procedure requires about six hours for complete sublimation but yields the feed metal in readily recoverable form with no increase in the oxygen content.

Table XI

Treatment of Nb-NbI_x Mixtures

Sample	O_2 in original Nb, ppm	Method of Treatment	O_2 in sample after treatment ppm
4A	32	conc. HNO_3+48% HF	Metal badly corroded, not analyzed
4B	32	2.5g KOH+0.25g I_2 in 50 ml. of water	Gas evolution on melting, not analyzed
4C	32	24% HF+76% conc. HNO_3 by volume	880
4D	32	Boiling conc. NaOH	Gas evolution on melting, not analyzed
10A	143	Boiled with dil. HNO_3 followed by 4.8% HF	310
10B	143	Boiled with dil. HNO_3 followed by 13% HF	470
10C	143	Boiled with conc. NaOH to which I_2 was added	1920

3.3 Thorium

3.3.1 Purification of Thorium by the Iodide Process (W. L. Larsen, D. E. Williams, O. D. McMasters, P. E. Palmer)

A Pyrex apparatus for the purification of thorium by the iodide process has been used to supply small research quantities of the metal.

3.3.2 Preparation by the Ca-Mg Reduction of ThF_4 (H. A. Wilhelm and R. L. Snyder)

The charges employed in this work are designed to prepare a low melting Th-Mg alloy and a low melting CaF_2-MgF_2 slag. Since the heat of reaction and the preignition added heat together are not sufficient for melting the products of the reaction, the separation of molten alloy and molten slag is obtained by a post-heating of the products. The thorium metal is recovered as a sponge from the alloy by vaporizing the magnesium in a subsequent vacuum heating treatment. Arc melting the thorium sponge gives dense thorium metal.

By carrying out the reduction under two atmospheres pressure of inert gas, alloys containing 1.6, 1.7, 1.8, 1.9 and 2.0 moles of magnesium per mole of thorium were successfully produced. A piece of $ThMg_2$ alloy was heated in vacuum to drive off the magnesium. The resultant sponge was arc melted and a section of the button given a cold rolling test. It withstood nearly 95% reduction in thickness on cold rolling without severe edge cracking.

3.3.3 Preparation by Mg Reduction of $ThCl_4$ (D. T. Peterson)

The development of the magnesium reduction of $ThCl_4$ as a method of preparing high purity thorium metal was reactivated. The method consists of the reduction of $ThCl_4$ with an excess of magnesium in an inert metal crucible to obtain a liquid thorium-magnesium alloy which is then heated under vacuum to remove the magnesium. The thorium sponge can be arc melted or induction melted to produce a solid ingot.

The previous work on this method indicated that the purity of the thorium was primarily influenced by the purity of the starting materials. Purification of $ThCl_4$ by sublimation under vacuum had not reduced the oxygen content to the expected level. An investigation of the separation of particulate impurities during sublimation showed the factors which govern the purity of the sublimation product, and the results were used to develop a more effective sublimation procedure for the purification of $ThCl_4$.

Thorium tetrachloride was purified by triple sublimation in a batch still under reduced pressure. In the second and third sublimations, the $ThCl_4$ vapors were contacted with thorium turnings to remove metallic chlorides such as $CrCl_3$, $FeCl_2$ and $MnCl_2$. By controlling the sublimation rate and the pressure in the sublimation still, the separation of ThO_2 and carbon was greatly improved. The sublimation still was loaded and unloaded in a glove box to prevent contamination by moisture.

The reductions were carried out in a tantalum crucible enclosed in a stainless steel tube. The charge consisted of 420 grams $ThCl_4$ and 140 grams of Mg. The reactants were mixed in the glove box, charged into the reduction apparatus and heated to 900°C for one hour under an atmosphere of argon. After cooling, the slag and thorium-magnesium alloy were broken out of the crucible and separated. The thorium-magnesium alloy was heated under vacuum in a titanium retort to 950°C for 4 hours. The dense thorium sponge which resulted was arc melted into buttons.

The changes which have been made in this reduction process have improved the purity of the thorium metal so that it is comparable to crystal

bar thorium. Analytical results and hardness values for two lots of metal prepared by this process are given in Table XII along with typical values for crystal bar thorium. The principal purity difference is the slightly higher oxygen content of the Mg-reduced thorium. The Mg-reduced thorium was purer than crystal bar thorium for several metallic elements. For a large number of metallic impurities the concentrations were below the range of present standard analytical methods.

Table XII

Analytical Results and Hardness of Mg-Reduced Thorium

Element	Mg-Reduced Thorium Sample A	Mg-Reduced Thorium Sample B	Crystal Bar Thorium
Carbon	128	136	80
Nitrogen	123	97	55-90
Oxygen	240	380	58
Hydrogen	3.8	3.4	3.5
Fe	16	14	20
Mn	1	1	20
Mg	30	20	20
Ca	20	20	20
Be	20	20	20
Si	20	25	50
Ni	20	20	--
Cr	20	20	--
Al	20	20	30
Hardness, RE	--	18	11
" , DPH		43	38

3.4 Yttrium (O. N. Carlson and F. H. Spedding)

The major research emphasis in this area during this period was on the improvement of the purity of the metal. Several different approaches were tried in attempts to remove oxygen from yttrium metal or to prevent the introduction of oxygen in processing. The approaches that were tried fall into one of four categories: (1) improvements in purity of ingredients and processing techniques (2) addition of carbon in vacuum arc melting step to remove CO from metal (3) electrorefining of yttrium and (4) extraction of oxygen from Y-Mg alloy with fused salts. Much of this work is described in the newly published report "Studies of the Preparation, Properties and Analysis of High Purity Yttrium Oxide and Yttrium Metal" by C. V. Banks, et al. This is a U. S. Atomic Energy Commission document, IS-1, July, 1959.

3.4.1 Improvements in Purity of Ingredients and Processing Techniques (F. A. Schmidt and J. A. Haefling)

It has been shown previously that the ingredients YF_3, $CaCl_2$, Ca or Li are principal sources of oxygen in yttrium metal. Experiments on the purification of calcium and lithium are described in detail in section 3.8 of this report. The $CaCl_2$ used as a flux in the reaction is a potential source of water and thus of oxygen. Yttrium of lower oxygen content was obtained with $CaCl_2$ which had been vacuum dried at 450°C followed by a treatment with hydrogen chloride gas at the same temperature. However, the actual oxygen content of the $CaCl_2$ that was purified in this manner is unknown.

The recent development of a quantitative method of analyzing for the oxygen content of YF_3 has shown that oxygen is present in amounts of 300 to 800 ppm in different batches of fluoride. Purification of yttrium fluoride was tried by fusing it in vacuo in a graphite crucible and by distilling it out of a graphite crucible in the presence of platinum at a temperature of 1700°C. Some purification in the fluoride was obtained by both methods.

The reactivity of the intermediate Y-Mg alloy toward atmospheric moisture and oxygen in the removal and crushing operations is a source of undetermined amounts of oxygen. A large steel dry box was constructed and equipped with facilities for loading and unloading the reduction retort, and for crushing and screening the alloy. This chamber can be completely evacuated and back-filled with an inert gas.

An alternate approach that was explored was the combination of the reduction and demagging operations into one heating step thus eliminating the handling and crushing of the alloy. The reductions were carried out in a flat, shallow titanium boat in which YF_3 was reacted with Ca or Li to form the low melting Y-Mg alloy. The alloy was allowed to solidify and the lower melting $CaCl_2$-CaF_2 or LiF slag was poured off. The system was then evacuated and the magnesium was removed from the alloy by vacuum sublimation. Although the alloy was in massive form most of the magnesium was removed by a prolonged heating period. The resulting sponge contained unremoved slag pockets, however, and the oxygen and fluorine contents varied considerably on samples from different regions and from run to run.

The need for improved vacuum conditions during the magnesium removal step called for a further look at the possibility of carrying this operation out at lower temperatures. This had always been done previously at 1150-1200°C. The yttrium-magnesium alloy was successfully demagged at 950°C under a pressure of 10^{-3} microns over a period of 30 hours. The interest in this lower temperature process comes from the ability to carry this out in a stainless steel retort in an electric resistance furnace. It eliminates the use of quartz vacuum tubes, ceramic insulation and induction heating and could be scaled up to large scale rather simply. The magnesium and calcium are removed to less than 100 ppm which gives a sponge product that is suitable for arc melting.

A demagging unit of this type capable of demagging 100 lbs. of alloy in one batch was assembled from exisitng equipment. A typical demagging cycle in this unit consisted of heating to 900°C and holding for 5 hours after which time the temperature was increased to 950°C where it was held for 24 hours. All of the yttrium sponge produced in this apparatus contained from 300 to 500 ppm oxygen.

A 12 lb. batch of yttrium sponge was sent to the Temescal Metallurgical Corporation for electron beam melting into ingot form. The sponge contained 400 ppm oxygen and 600 ppm fluoride. The double melted ingot contained approximately the same amount of oxygen but the fluoride content was lowered to 40 ppm.

3.4.2 Attempts at Removing Oxygen from Yttrium Metal by Carbon Addition. (F. A. Schmidt)

Since oxygen can be removed from yttrium metal as CO in the vacuum fusion analysis, it appeared possible that similar results could be obtained by vacuum arc melting. A stoichiometric amount of carbon was added to the sponge prior to vacuum arc melting. The results of this series of experiments are presented in Table XIII. There was no measurable decrease in oxygen or significant loss in the amount of carbon added.

Table XIII

Experiments on Removal of Oxygen by Carbon Addition

Yttrium Sponge Number	Treatment	Arc melting Conditions	Analysis of Final Metal (ppm)		
			C	F	O
39-79M(b)C	No C addition	Reduced pressure	650	492	3400
"	No C addition	Vacuum	630	576	3700
"	Sponge melted by ind. heating in graphite	Vacuum	1166	362	3480
"	C added during sponge compacting	Reduced pressure	3269	290	3780
"	C added to reduction	Vacuum	578	424	3550

3.4.3 Electrorefining of Yttrium Metal (F. A. Schmidt)

Experiments on the electrorefining of yttrium metal employing a fused salt electrolyte were instigated. A six-inch electrorefining cell consisting

of a stainless steel retort, titanium crucible and two water cooled electrodes was constructed and used in the electrolysis experiments.

Since the nature of the deposit is important in electrorefining, runs were made in order to establish the conditions whereby coarse crystals can be obtained from which the salt can be completely removed. Fused salt baths containing mixutres of $CaCl_2$-YF_3 and $CaCl_2$-YCl_3 were used as electrolytes. Six-inch rods of yttrium metal were attached to the water cooled electrode and used as the anode and cathode. Experiments indicated that a high current density from the chloride electrolyte is detrimental to coarse crystal growth. The coarse yttrium deposits so far obtained do not show a significant decrease in the oxygen content of the metal.

3.4.4 Purification of Y-Mg Alloy by Fused Salt Extraction (J. A. Haefling and F. A. Schmidt)

The most successful approach to the purity problem was found to be the extraction of oxygen from the Y-Mg alloy with fused salts. The results of a large number of experiments are given in Table XIV in which the reduction process employed, the extractant used, and the oxygen content of the metal before and after extraction are tabulated in the various columns.

Summarizing the results of these experiments, it is noted that the oxygen content is drastically lowered by extraction with $YF_3 \cdot CaCl_2$, $YF_3 \cdot LiF$ and $CaF_2 \cdot LiF \cdot YF_3$ mixtures. The amount of extractant is critical but beyond that point there is little advantage in using greater

Table XIV

Experiments on Purification of Yttrium by Fused Salt Extraction

	Reduction Procedure	Extractant	Ppm Oxygen in Metal Prepared	Ppm Oxygen in Metal Before Extraction
1.	Lithium reduction of yttrium fluoride	lithium-fluoride-yttrium fluoride	580	1130
2.	"	calcium chloride-yttrium fluoride	770	1130
3.	"	65% excess yttrium fluoride in reduction	720	1130
4.	Extractant from (1) reduced with Ca	----	1180	----
5.	Extractant from (2) reduced with Ca	----	3260	----
6.	Slag containing excess yttrium fluoride from (3) reduced with Ca	----	3480	----
7.	Calcium lithium reduction of yttrium	Calcium fluoride-lithium fluoride-yttrium fluoride	630	1920
8.	"	calcium chloride-yttrium fluoride	510	1920
9.	Extractant from (7) reduced with Ca Li	----	4140	----
10.	Extractant from (8) reduced with Ca	----	3760	----
11.	Calcium reduction of YF_3-$CaCl_2$ mixture	calcium chloride-yttrium fluoride	730	2600
12.	Extractant from (11) reduced with Ca	----	3350	----

Table XIV con'd

	Reduction Procedure	Extractant	Ppm Oxygen in Metal Prepared	Ppm Oxygen in Metal before Extraction
13.	Calcium reduction of	stoichiometric ingredients used in reduction	2740	2600
14.	"	13% excess yttrium fluoride	1650	2600
15.	"	50% " "	1270	2600
16.	"	yttrium fluoride-calcium chloride; extracted three times	370	2230
17.	"	calcium chloride	1750	2230
18.	"	lithium fluoride	1920	1780
19.	"	yttrium chloride	1350*	2000

* Only 200 grams of yttrium chloride were used.

volumes of extractant. Multiple extractions result in somewhat purer material but the first extraction is the most significant one. Extraction with pure LiF or $CaCl_2$ does not lower the oxygen content and may in fact, raise it. In some experiments the extractant mixture was subsequently reduced and the resulting metal analyzed for oxygen. In all cases the metal was much higher than for a standard reduction verifying the transfer of oxygen to the salt phase.

As a result of the above survey a series of extractions was run using mixtures of YF_3 and $CaCl_2$ in which the weight of one ingredient was varied while the other was held constant. Table XV gives the results of these experiments. From these data it appears that a minimum amount of YF_3 is

Table XV

Effect of Variations of YF_3:$CaCl_2$ Ratio in Extractant Mixture

Exp. No.	Wt. of alloy Extracted	Wt. of $CaCl_2$ Used	Wt. of YF_3 Used	Stirring Time	Ppm O_2 in Y Ingot
1	1200 g.	1350 g.	1650 g.	10 min.	520
2	"	"	1150 g.	"	530
3	"	"	650 g.	30 min.	820
4	"	"	"	10 min.	780
5	"	"	150 g.	"	2100
6	"	"	650 g.	30 min.	600
7	"	530 g.	"	"	680
8	"	400 g.	"	"	520
9	"	300 g.	"	"	600
10	"	200 g.	"	"	720
11	"	100 g.	"	"	670

required but that amounts in excess of this have a decreasingly small effect. The amount of $CaCl_2$ used is unimportant as long as enough is used to flux the fluoride salt.

As was described in an earlier report[1] it was known that oxygen from

1. Semi-Annual Summary Research Report in Metallurgy, U.S.A.E.C. Report, No. ISC-977, July-December 1957, p. 27.

any of the above compounds is introduced quantitatively into the alloy during the reduction step. These contaminated charges were then extracted with fresh YF_3 and $CaCl_2$. As is shown in Table XVI in all cases the added oxygen was extracted by the fused salt along with other oxygen present.

Table XVI

Effect of $YF_3 \cdot CaCl_2$ Extractant on Various Oxide Additions to Y-Mg Alloy

1000 Ppm Oxygen Added as	Approx. Total Ppm Oxygen in Alloy	YF_3 in Extractant Mixture	Ppm O_2 in Y Ingot
no addition	2000	650 g.	500
MgO	3000	1000 g.	550
CaO	3000	1000 g.	520
Y_2O_3	3000	1000 g.	470
YOF	3000	1000 g.	485

The amount of oxygen in the alloy and in the YF_3 used in the extractant mixture was also varied. It was found that greater amounts of YF_3 were necessary in the extractant when the alloy or the YF_3 contained large quantities of oxygen. Table XVII shows the results of these experiments.

Five large scale (100 pound) reductions and extractions were run in order to prepare about 400 lbs. of low oxygen Y metal for evaluation purposes. The resulting metal contained an average of about 400 ppm oxygen and 600 ppm fluoride.

Table XVII

Effect of Purity of YF_3 on Extractant Mixture

Estimated Oxygen in Alloy (ppm)	Estimated Oxygen in YF_3	Wt. of YF_3 in Extractant	Ppm Oxygen in Y Ingot
5000	400	1000 g.	650
5000	400	500 g.	1370
2000	2200	1000 g.	630
2000	2200	500 g.	1120
2000	400	500 g.	550

Further work was done using YCl_3 as an extractant, both as the first extractant salt and as a second extractant on alloy that had previously been treated with fused YF_3-$CaCl_2$. The results of these experiments (see Table XVIII) indicate that the fluoride content of the metal is substantially reduced by the use of YCl_3 extractant, and it appears to be as effective as YF_3 in removing oxygen from the metal. The principal disadvantages in its use lie in the difficulty in preparing it in quantity and high purity and in its hygroscopic nature.

3.4.5 Evaluation of Yttrium Metal Ingots (F. A. Schmidt and J. A. Haefling)

Some correlation between BHN hardness and oxygen content was noted on yttrium metal in the arc-cast state. Brinell hardness numbers of 45 to

Table XVIII

Use of YCl_3 as Extractant Salt

Extraction Procedure	Impurities in Yttrium After Extraction			
	C	N	O	F
1. YCl_3 as 1st stage extractant	105	15	575	360
2. YCl_3 as 2nd stage extractant	95	20	165	120
3. Repeat of 2 above in tantalum crucible	90	20	200	70

55 were obtained from metal containing 400-700 ppm oxygen, while BHN values of 85-100 were obtained from metal containing 3000-4000 ppm oxygen. However, this correlation was not found to be present after the samples had been vacuum annealed at 950°C for 2 1/2 hours and slow cooled. In all cases the hardness values obtained after the annealing treatment were below BHN 55.

A series of arc-melted specimens were vacuum annealed and quarter inch thick sections taken from these were cold rolled to greater than a 95% reduction in thickness. Table XIX gives the analytical data on these ingots. Ingots F-73 and F-74 were sent out for extrusion tests. It was reported that they were satisfactorily extruded at 550°F. A 1" x 1" x 1.015" section of C-332 was hot rolled (1000°F) to a 95% reduction in thickness without edge cracking. Another specimen of this ingot was cold rolled 95% with slight edge cracking.

Table XIX

Analysis of Ingots Used in Rolling and Extrusion Tests

Ingot No.	Wt. lbs.	C	N	Ca	Mg	O	H	F	BHN (as annealed)
F- 73	7.63	67	77	10	30	550	115	676	37.5
F- 74	7.65	66	51	10	185	570	10	682	35.9
C-332	5.76	143	87	10	---	490	75	624	36.2

Ten yttrium-alloy ingots were prepared for evaluation of their fabricability by the General Electric group at Cincinnati. The yttrium sponge used in these ingots was prepared by a single extraction with a $YF_3 \cdot CaCl_2$ mixture. The alloying agents were added to the yttrium sponge during the compacting operation. The individual compacts were arc melted under 40 mm of helium into 2 1/2" diameter ingots. These were then vacuum arc melted into the 3 1/2" diameter five pound ingots listed in Table XX.

3.5 Uranium Metal by Carbon Reduction of Uranium Oxide (H. A. Wilhelm and E. P. Neubauer)

The work on the carbon reduction of UO_2 toward increased yield and reduced carbon content of the metal has met with only limited success. In order to gain further knowledge of the problems involved, a more detailed investigation of the mechanism of the reduction reaction was undertaken.

Table XX

Alloy Ingots Prepared for Evaluation by Genral Electric

Ingot No. (vac. melt)	Alloy Agent	Analyzed Alloy Content w/o	Wt. of Ingot (lbs)	BHN 500 Kg as Arc Melt	BHN 500 Kg as Annealed	Ppm Oxygen
C-343-B	--	----	5.5	49.5	36.4	600
C-343-B	Cr	0.53	5.1	51.8	38.1	570
C-334-B	Cr	1.44	4.5	47.4	40.5	440
C-335-B	Cr	2.83	5.2	53.6	48.9	520
C-336-B	Cr	4.82	5.4	62.7	52.2	510
C-337-B	Ge	0.9	4.8	51.6	43.6	510
C-338-B	Nb	1.0	5.6	45.3	40.4	680
C-339-B	Nb	1.5	5.4	46.3	40.1	680
C-340-B	V	0.5	5.4	41.4	43.2	630
C-341-B	V	2.4	5.3	59.4	51.7	680
C-342-B	V	3.15	5.6	57.5	50.1	830

The procedure followed for getting data was to run the reaction using varying amounts of carbon and to halt the reaction before it reached completion. For each amount of carbon used there was a temperature at which the rate of CO evolution fell off markedly. When this rate decrease occurred, the reaction was halted. The products were gray, sintered cakes of UO_2 and UC.

Indications are that the carbon reduction of UO_2 to metal, proceeds stepwise with a solid-solid reaction between UO_2 and UC occurring at one stage to give the overall reaction,

$$UO_2 + 2C \rightarrow U + 2CO.$$

The sintered cake of UO_2 and UC was found to have an electrical conductivity comparable to graphite. This meant that it should be possible to induction heat the sintered cake without the use of a graphite heater. This was attempted with the sintered cake packed in UO_2 which acted as both crucible and insulation. Because of the small diameter of the sintered cakes tested so far, temperatures sufficiently high to complete the reaction have not yet been reached.

Another approach to the self-induction heating that was tried was to complete the reduction reaction in a graphite crucible. The metallic biscuit, consisting of U and UC, was packed in UO_2. It was hoped that the UC in the metal would react with the insulation to yield high purity metal. Melting did occur and the molten metal which was set into motion by the induced currents formed what appeared to be a cermet with the UO_2 insulation.

At the temperatures needed to complete the reduction reaction, the volatility of UO_2 is so high that it is believed partly responsible for the low yields of metal. Attempts have been made to get the reaction to go to completion at a lower temperature by introducing certian agents in the charge, but so far no favorable results have been obtained with this approach.

During a number of the experiments on the carbon reduction of UO_2, the product metal was lost because inferior quality crucibles were used. It was felt that a further investigation of the preparation of UO_2 crucibles should be undertaken. Some improvements in crucible quality have already been obtained. Some of the developments of this study might possibly be applicable to preparation of ceramic fuel elements for nuclear reactors.

3.6 Preparation of Tantalum Metal (H. A. Wilhelm and C. B. Hamilton)

The method of producing high purity tantalum by the carbon reduction of tantalum pentoxide at high temperature in a vacuum is being studied in some detail. The best metal obtained so far by this method followed by arc melting contained 250 ppm carbon and 53 ppm oxygen.

By using less than stoichiometric amounts of carbon in the reduction, the residual oxide can be boiled off as TaO_2. To adequately boil off this oxide, the metal should be held at about 2400°C in a vacuum. It is rather difficult to hold this high temperature without getting carbon contamination from graphite if used as a container in induction heating. Attempts to decrease the vaporization of the carbon by forming a tantalum carbide layer on the graphite were unsuccessful. The best protection is a shield of tantalum metal of at least 10 mils thickness between the walls of the graphite heater and the tantalum sponge.

The use of resistance heating on carbon-reduced tantalum sponge gives some promise in removing any oxygen which does not react below

2000°C. The temperature is easily raised to 2400°C or higher without fear of carbon contamination when a pressed bar of the sponge is heated by the electrical resistance.

When a temperature vs. pressure plot is run in a reduction experiment, three pressure peaks appear. The first appears between 1200°C and 1500°C and is due to the major part of the reaction. Various lots of Ta_2O_5, from different sources, give their maximum reactions at different temperatures in this range. The calcining temperature of the tantalum pentoxide appears to be a factor determining the temperature at which the carbon starts reacting. The higher the temperature the tantalum pentoxide has been calcined, the higher the temperature required for the maximum reaction rate in this first stage.

The second peak is around 1800°C and the third is at about 2200°C. To explore the possible bases for these peaks in gas evolution, a series of reductions were run in which the reactions were stopped at different temperatures. X-ray diffraction patterns were made of each sample. It was noted that in the reduction stopped before the 1800°C peak, there were lines indicating tantalum carbide, but in samples taken above the 1800°C peak no carbide lines were detected. There is evidence then that the major reaction up to about 1700°C is between carbon and oxide to give some tantalum carbide, while the major part of the reaction at around 1800°C is between carbide and oxide. When an excess of carbon was employed in the charge, the 2200°C peak was eliminated. The 2200°C peak is assumed to be connected with the volatilization of excess TaO_2 which reacts with the carbon heater to give a pumpable gas.

The addition of another metal to the reduction charge could possibly act as a scavenger for oxygen if the metal oxide has the proper volatility with respect to the assumed TaO_2. Such a metal oxide could possibly permit a lower finishing temperature for the preparation of good metal. A number of metal oxides were added to charges of Ta_2O_5 and carbon, and tested as possible scavengers. The reductions were made with a deficiency of carbon and with an excess of carbon. Only TiO_2, SiO_2 and possibly MnO_2, with added carbon, showed any promise of behaving in the desired manner. Manganese was tested further and showed to have no scavenger tendencies in the tantalum. Work is continuing with the titanium and silicon additions to the charge.

3.7 Purification of Calcium and Lithium by Vacuum Sublimation and Distillation. (O. N. Carlson, J. A. Haefling and F. A. Schmidt)

The preparation of high purity calcium by vacuum sublimation techniques was resumed. Previous small scale experiments had shown that magnesium can be removed quantitatively by vacuum sublimation at 800°C for a prolonged period. Chemical analysis indicated that the magnesium content of the metal had been decreased only slightly from that of the crude starting material which contained 0.3 w/o magnesium.

Lithium is used as a reductant in the experimental yttrium reduction work. Oxygen and nitrogen present in commercially available lithium are undesirable impurities in yttrium metal. Experiments on the purification of lithium metal by vacuum distillation indicate that nitrogen is removed, but that complete removal of oxygen by distillation is impossible, probably due

to the volatility of lithium oxide. A series of experiments was run in which various additions were made to the lithium during distillation in an effort to preferentially getter the oxygen. The distilled and condensed lithium was then used as the reductant on a series of yttrium fluoride reductions and the yttrium metal was analyzed for oxygen. The results of these experiments are presented in Table XXI. The addition of 5 w/o calcium was found to bring about the greatest decrease in oxygen. This is attributed to the formation of a stable, non-volatile CaO from which the lithium distills away. The calcium which was added is likewise left behind in the residue since the distillation is carried out at temperatures well below the boiling point of calcium.

Table XXI

Gettering Effect of Various Additives on Lithium During Vacuum Distillation

	Y Metal Obtained by Reduction with Distilled Li	
	Ppm O	Ppm N
Lithium (used as received)	2640	135
" " " "	2750	250
" " " "	3750	520
Filtered lithium	1960	95
Ti sponge added	2300	100
Y sponge added	2650	132
Zr sponge added	2200	110
YF_3 added	2270	90
10 w/o Ca added	1680	95
10 w/o Ca "	1630	75
10 w/o Ca "	1300	100

4. Alloy Investigations

4.1 Phase Relations and Thermodynamic Properties of the Th-Zn System.

4.1.1 Solubility of Thorium in Zinc. (P. Chiotti and K. Gill)

Experimental determinations of the thorium content in liquid zinc equilibrated with an excess of solid Th_2Zn_{17} at various temperatures have been completed. The results obtained are summarized along with the results of thermal analyses for the liquidus in Fig. 3. Values taken from the curve in Fig. 3 are given in Table XXII.

Table XXII

Solubility of Thorium in Zinc

°C	a/o Th	w/o Th
419	0.00073	0.0026
500	0.0061	0.022
600	0.053	0.19
700	0.280	0.99
800	1.10	3.79
900	3.40	11.12
1000	8.80	25.52

4.1.2 Zinc Vapor Pressure and Thermodynamic Properties of Zn-Th Alloys (P. Chiotti and K. Gill)

The vapor pressure of zinc over two-phase alloys consisting of $Th-Th_2Zn$, $Th_2Zn-ThZn_2$, $ThZn_2-ThZn_4$ and $ThZn_4-Th_2Zn_{17}$ was

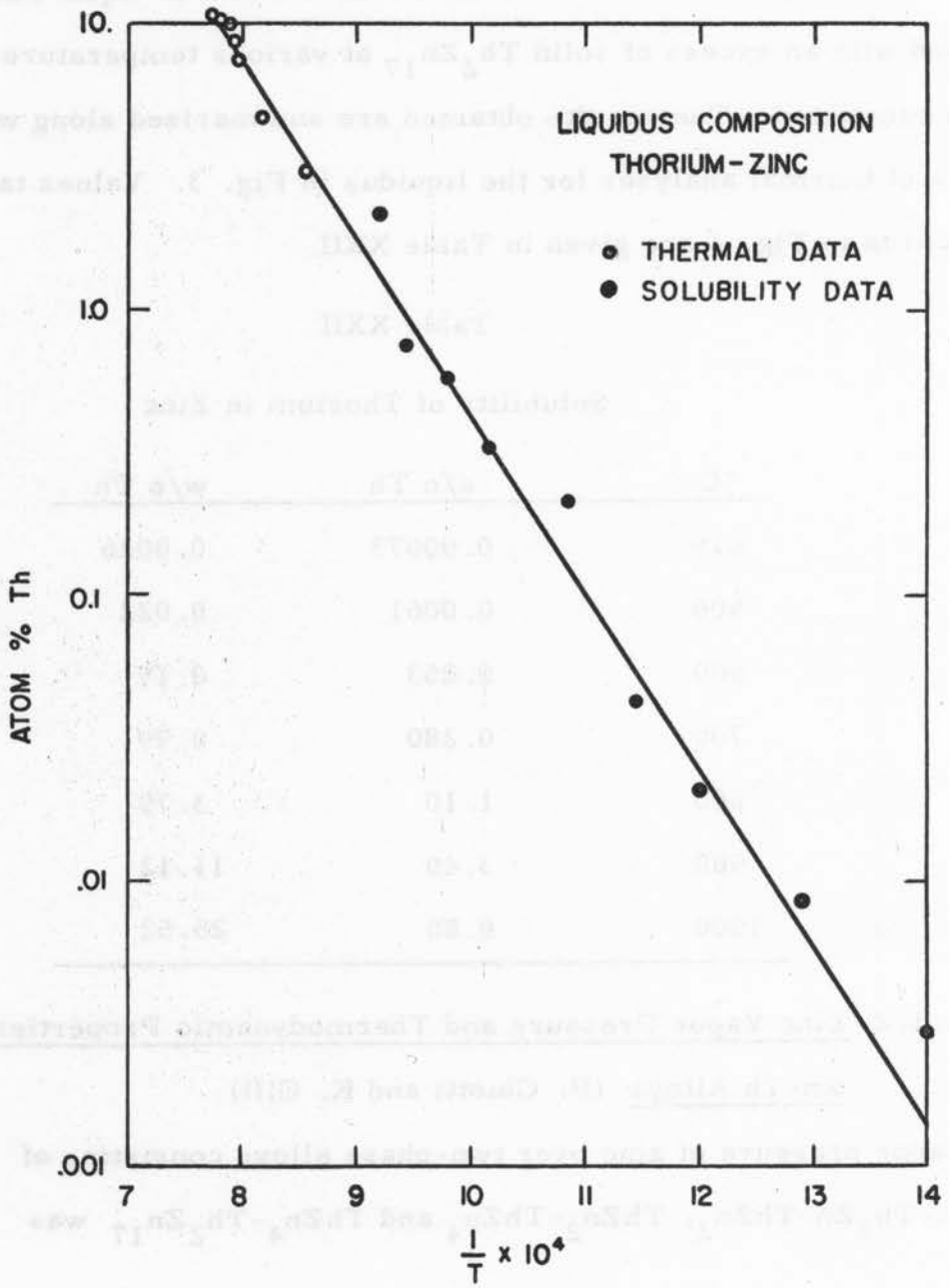

Fig. 3. Solubility of thorium in liquid zinc.

measured as a function of temperature by the dew-point method. The data obtained were fitted to relations of the type,

$$\log P_{atm} = aT^{-1} + b,$$

and are summarized in Table XXIII. Additional work is in progress to improve the precision of the method of measurement and to further check these data. Consequently some minor adjustment of the values for the constants tabulated in Table XXIII and the calculated thermodynamic properties may be necessary.

Table XXIII

Zinc Vapor Pressure as a Function of Temperature for Four of the Solid Two-Phase Regions of the Th-Zn System

$$\text{Log } P_{atm} = aT^{-1} + b$$

Equilibrium Phases	a	b	Temp. Range °K
Th-Th_2Zn	-9755	6.40	875-1215
Th_2Zn-$ThZn_2$	-9286	6.54	880-1180
$ThZn_2$-$ThZn_4$	-8298	6.33	800-1200
$ThZn_4$-Th_2Zn_{17}	-7106	5.78	855-1190

From the relations for the vapor pressure, the temperature at which the zinc pressure is one atmosphere is calculated to be 1252, 1147, 1037 and 957, respectively, for the regions in the order tabulated in Table XXIII. These calculations are valid except for the first two temperatures. The

phase diagram, (see ISC-1050), shows that the temperatures 1252 and 1147°C lie above the respective eutectic temperatures, 1040 and 945°C, for the Th-Th_2Zn and Th_2Zn-$ThZn_2$ regions. The vapor pressure equations for these two solid regions are not valid above the eutectic temperatures. However, an alloy containing 89 w/o thorium would be expected to have a zinc pressure of somewhat less than one atmosphere at 1252°C.

The vapor pressure equations given in Table XXIII can be used along with known relations for the free energy of vaporization, for pure zinc to calculate the standard free energy, enthalpy and entropy of formation for the Th-Zn compounds. Results of these calculations are summarized in Table XXIV. Some small changes in these values may be necessary since some of the vapor pressure data is being rechecked.

4.1.3 Crystal Structures of Th-Zn Compounds. (P. Chiotti and E. Ryba.)

Four intermetallic compounds exist in the Th-Zn system which correspond to the formulas Th_2Zn, $ThZn_2$, $ThZn_4$ and Th_2Zn_{17}. The compound Th_2Zn was found by Baenziger, et al.[2] to be body-centered tetragonal, space group D_{4h}^{18}-I4/mcm, with a = 7.60 Å and c = 5.64 Å. The compound Th_2Zn_{17} was found by Makarov and Vinogradov[3] to be

2. N. C. Baenziger, R. E. Rundle and A. I. Snow, Acta Cryst. 9, 92 (1956).

3. E. S. Makarov and S. I. Vinogradov, Kristallografiya 1, 634-643 (1956).

Table XXIV

Thermodynamic Properties of the Compounds in the Th-Zn System

		$-\Delta F°$ KCal/mole	$-\Delta H°$ KCal/mole	$-\Delta S°$ cal/mole/degree
Th_2Zn				
25°C	298°K	13.2	13.4	.78
500	773	12.3	15.9	4.7
600	873	11.8	16.2	5.1
700	973	11.3	16.5	5.4
800	1073	10.7	16.8	5.7
$ThZn_2$				
25°C	298°K	22.9	23.7	2.5
500	773	20.6	28.6	10.4
600	873	19.5	29.2	11.1
700	973	18.4	29.8	11.8
800	1073	17.1	30.5	12.4
$ThZn_4$				
25°C	298°K	36.2	37.2	3.4
500	773	23.3	47.1	19.1
600	873	30.3	48.3	20.6
700	973	28.2	49.6	22.0
800	1073	25.9	50.9	23.3
Th_2Zn_{17}				
25°C	298°K	89.8	86.4	-11.5
500	773	85.8	128.4	55.1
600	873	79.9	133.6	61.4
700	973	73.5	138.9	67.2
800	1073	65.5	144.3	73.4

rhombohedral, space group D_{3d}^5-$R\bar{3}m$, with hexagonal lattice constants a = 9.03 Å and c = 13.20 Å. Makarov and Gudkov[4] in a study of the Th-Zn compounds, report in addition to the last three compounds listed above, presumably two other compounds $Th_{2+x}Zn$ and Th_4Zn_7 or Th_8Zn_{15}. Metallographic and thermal analyses made in our investigation show only the compound Th_2Zn. They found $ThZn_2$ to be hexagonal, AlB_2 type, with a = 4.20 Å and c = 4.17 Å, and $ThZn_4$ to be body-centered tetragonal, $BaAl_4$ type, with a = 4.26 Å and c = 10.4 Å.

X-ray data obtained with single crystals of $ThZn_4$ have been consistent with the structure reported by Makarov and Gudkov. Back-reflection powder patterns indexed on the basis of $\sin^2\theta$ values for all possible hkl reflections, calculated from the approximate lattice constants given by Makarov and Gudkov, gave refined lattice constants of a = 4.273 Å and c = 10.395 Å. Tentative results on $ThZn_2$ do not appear to be consistent with the structure reported by the same authors. Further work on the $ThZn_2$ structure is in progress.

4.2 Solubility of Uranium in Zinc. (P. Chiotti & H. Shoemaker.)

The solubility of uranium in zinc is of interest in the pyrometallurgical process proposed for the purification of uranium described elsewhere in this report. Zinc solutions were equilibrated with excess U_2Zn_{17} (solid phase) at various temperatures, and samples of the saturated liquid were

---

4. E. S. Makarov and L. S. Gudkov, Kristallografiya 1, 650-656 (1956).

taken for analyses. The results obtained are shown plotted in Fig. 4. Values taken from this curve are listed in Table XXV.

Table XXV

Solubility of Uranium in Zinc

Temp. °C	a/o	w/o
425	0.0012	0.0043
500	0.0090	0.033
600	0.076	0.277
700	0.41	1.48
800	1.62	5.66
900	5.10	16.4
1050±25	10.53	30.0

4.3 Thorium-Yttrium Alloy System (O. N. Carlson and D. T. Eash)

The investigation of the thorium-yttrium alloy system was completed and a terminal report written on this work. A detailed description of the work is given in the doctoral thesis of D. T. Eash which was entitled "Thorium-Yttrium Alloy System". A condensation of this work is given in a journal paper entitled "Investigation of the Thorium-Yttrium System" by D. T. Eash and O. N. Carlson that has been accepted for publication in the Trans., ASM, Vol. 52, 1960.

A summary of this work is given below.

1. Complete solid miscibility exists at high temperatures.
2. An allotropic transformation from HCP to a BCC structure occurs in yttrium at 1490°C.
3. A eutectoid reaction takes place at 1375°C and 25 w/o Y.
4. The room temperature terminal solid solubility limits of α (Th) and α (Y) regions are approximately 20 and 30 a/o Y, respectively.

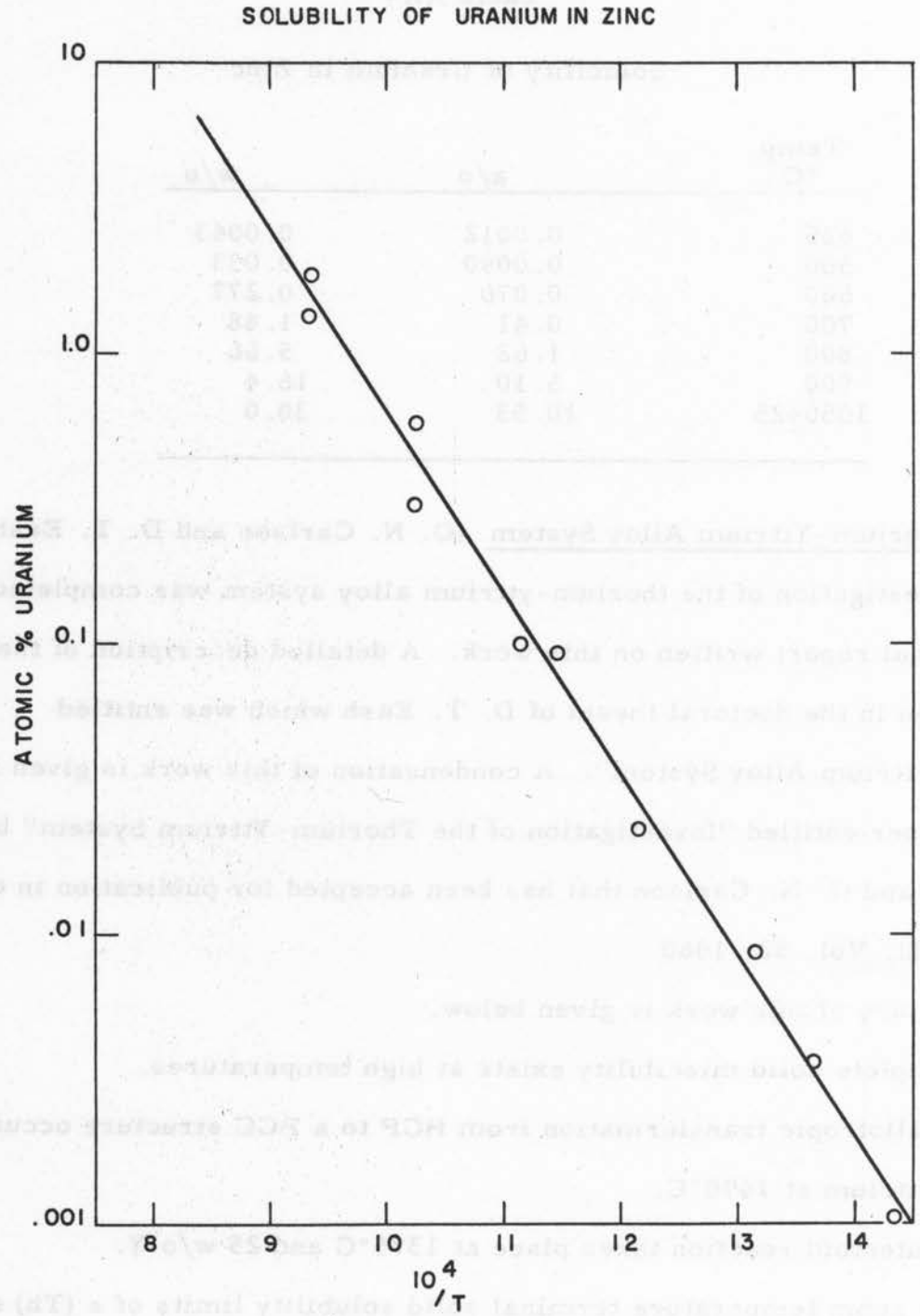

Fig. 4. Solubility of uranium in liquid zinc.

5. The corrosion resistance of yttrium and of thorium in boiling water was not significantly improved by alloying. The air oxidation properties of thorium-yttrium alloys were determined at 250°C and 500°C. The addition of yttrium to thorium tends to reduce its rate of air oxidation at both temperatures.
6. The yield strength of thorium was noticeably decreased by the addition of the first 10 w/o of yttrium. The percent elongation decreases sharply with the addition of 1 w/o Y but increases to a maximum, that is greater than that of the bomb-reduced thorium, at a 10 w/o Y addition. The reduction in area follows a similar trend.

4.4 Tantalum-Zirconium System (W. L. Larsen and D. E. Williams)

Although the formal investigation of this system had been completed previously, some of the minor points of the phase diagram were studied during this period.

An effort was made to locate more precisely the minimum in the solidus by a metallographic examination. The as-cast microstructures did not, however, reveal a positive indication of the minimum.

Specimens of the 2, 3, and 5 w/o tantalum alloys were reduced about 50% by cold-rolling and were heated to 750°C for periods of 1/4, 1, 10, and 100 hours. Metallographic study indicated that the 2, 3, and 5 w/o tantalum alloys had recrystallized after one hour at 750°C.

A diffusion couple of tantalum and zirconium was prepared and heated in vacuum at 750°C for 950 hours. After examination the couple

was reheated to 1300°C and held for 600 hours. Metallographic examination of the specimen revealed no intermetallic compounds.

Samples of the 90 and 95 w/o tantalum alloys were helium-quenched from 1200°C. Examination of the microstructures of the quenched alloys indicated the solubility limit to be between the two compositions at 1200°C.

4.5 Additions of Magnesium to Thorium (J. F. Smith, W. L. Larsen, D. E. Williams and W. H. Pechin)

Due to the failure to obtain homogeneous alloys notwithstanding the several methods and many attempts undertaken, the investigation of the thorium-rich portion of the thorium-magnesium system has been discontinued.

4.6 Yttrium-Niobium Alloy Investigation (O. N. Carlson, W. L. Larsen, V. C. Marcotte and D. E. Williams)

The electrical-resistance vs. temperature data collected during this period were somewhat inconsistent. Runs on the 30, 95, and 98 w/o niobium alloys gave curves which exhibited breaks at 1400°C, the tentative eutectic temperature. The resistance curve of the 10 w/o niobium alloy did not show an anomaly until a temperature of 1500°C was reached. The data obtained from the 5 w/o niobium alloy produced a curve which broke sharply at 1400°C after several discontinuities at lower temperatures. The present knowledge of the phase diagram is insufficient for complete interpretation of these results.

Liquidus determinations are being made by placing an yttrium niobium alloy in a niobium crucible and heating to a temperature above the melting point of the alloy. After the reaction between the alloy and the niobium

crucible reaches equilibrium, the crucible and its contents are quenched. The analysis of the equilibrium mixture gives the composition coordinate of a point on the liquidus curve at the temperature of the quench. Several yttrium-rich alloys have been treated in this manner but no reliable results have been obtained.

X-ray diffraction patterns were prepared from powder specimens of the 2, 5, 70 and 90 w/o yttrium alloys as well as unalloyed yttrium and niobium. The powders had been heated in vacuum to 600°C, held for one week and cooled slowly to room temperature. The X-ray data indicate no terminal solubility at room temperature.

4.7 Uranium-Rhenium Alloy Investigation (J. F. Smith, W. L. Larsen, R. J. Jackson and D. E. Williams)

The uranium-rhenium system is being investigated by various standard techniques. A tentative constitutional diagram is presented in Fig. 5.

The presence of the intermediate phase, Re_2U, has been established. This phase melts congruently at 2200 $\pm$ 75°C and exhibits an allotropic transformation at 180 $\pm$ 2°C. Efforts to determine the structure of the Re_2U compound by powder and single crystal X-ray diffraction techniques have not yielded satisfactory results. However, the single crystal work indicated the room-temperature structure is orthorhombic or tetragonal and has a rather large unit cell. The high-temperature structure is believed to be hexagonal.

There are two eutectic reactions, one between the intermediate phase, Re_2U, and each of the two terminal solid solutions. These reactions occur

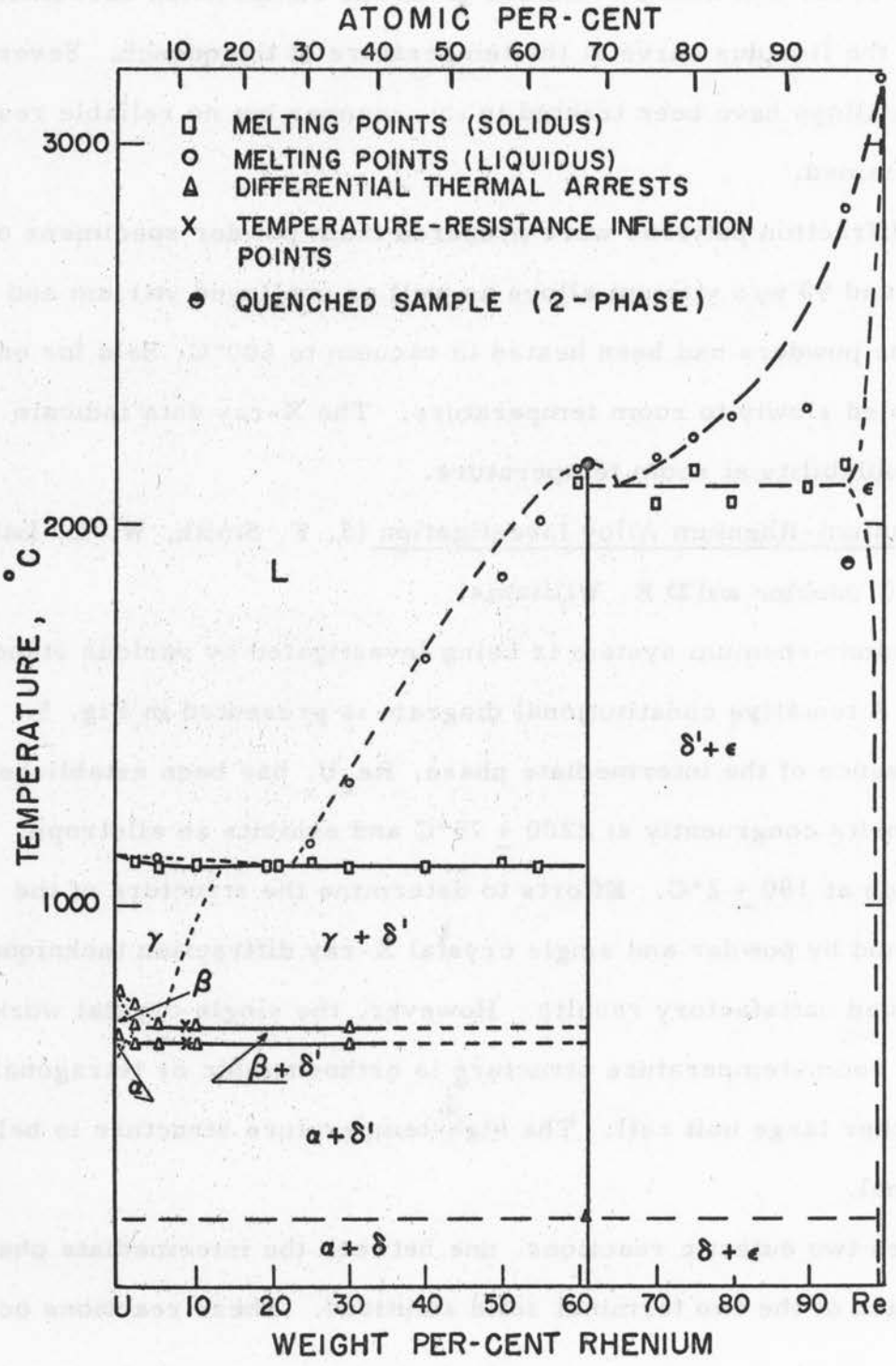

Fig. 5. Tentative uranium-rhenium phase diagram.

at 1104 ± 3°C and 2100 ± 60°C at compositions in the neighborhood of 20 and 65 w/o rhenium, respectively.

Two eutectoid reactions exist due to the solid transformations in uranium. The alpha-beta and beta-gamma eutectoid horizontals occur on heating at 640 ± 5°C and 679 ± 5°C, respectively. The eutectoid compositions are not known precisely but their probable locations are shown in Fig. 5.

Preliminary metallographic results indicate only limited solubility in all regions of the diagram including the intermediate phase, Re_2U. The solubility of rhenium in gamma uranium is an exception and may exceed 10 w/o at the eutectic temperature.

The as-cast alloys as a whole do not appear amenable to fabrication. The alloys of intermediate composition are brittle because of the influence of the Re_2U compound. The rhenium-rich alloys, while somewhat ductile, work-harden very rapidly and require frequent intermediate annealing. Rapidly cooled alloys containing about 10 w/o rhenium are relatively ductile. This ductility is believed to be due to the retention of the gamma phase.

4.8 Thorium-Molybdenum Alloy Investigation (W. L. Larsen, D. E. Williams and P. E. Palmer)

The investigation of the solubility limits of the thorium-molybdenum system is being continued. The maximum solubility of thorium in molybdenum is about 10 w/o while that of molybdenum in thorium is less than 2 w/o at the proposed eutectic temperature, 1400°C. There is no detectable solid solubility

on either side of the diagram at room temperature. High temperature X-ray diffraction techniques are to be applied to this alloy investigation for more exact solubility determination.

4.9 Crystallographic and Phase Relationships of the Nickel-Zirconium and Nickel-Hafnium Systems (W. L. Larsen, J. F. Smith and M. E. Kirkpatrick)

The structure determination of the intermetallic compound $Ni_{10}Zr_7$ is nearing completion. Weissenberg and precession photographs show the unit cell to be orthorhombic with $a_o = 9.22\text{Å}$, $b_o = 9.34\text{Å}$, and $c_o = 12.49\text{Å}$. This structure contains four formula weights per unit cell. The space group, as determined from nonextinction data, is P_{bca} with the special 4-fold positions (0, 0, 0; 1/2, 1/2, 0; 0, 1/2, 1/2; 1/2, 0, 1/2) occupied by zirconium atoms and the general 8-fold positions ($\pm$[x, y, z; 1/2+x, 1/2+y, $\bar{z}$; $\bar{x}$, 1/2+y, 1/2-z; 1/2-x, $\bar{y}$, 1/2+z]) occupied by three sets of zirconium atoms and five sets of nickel atoms.

A trial structure has been postulated from two- and three-dimensional Patterson projections. A two-dimensional Fourier projection on the (001) plane has yielded x and y parameters in close agreement with those postulated. A least squares refinement using visually judged hk0 intensity data has resulted in a reliability factor, $R = \frac{\Sigma|F_o| - |F_c|}{\Sigma|F_o|}$, of 12.10%. Table XXVI lists the x and y parameters obtained by the least squares refinement. The z parameters for this structure are only partially known at this time.

Table XXVI

x and y Parameters of $Ni_{10}Zr_7$

Parameter	Atom	x	y
P_o	Zr*	0	0
P_1	Zr	0	0
P_2	Zr	0.259	0.250
P_3	Zr	0.314	0.317
P_4	Ni	0.014	0.206
P_5	Ni	0.014	0.295
P_6	Ni	0.293	0.005
P_7	Ni	0.207	0.995
P_8	Ni	0.114	0.109

* Four-fold set, all others listed are eight-fold sets.

Recent work on the nickel-zirconium phase diagram has revealed the existence of a compound between the NiZr and $Ni_{10}Zr_7$ compounds. The newly discovered compound has been tentatively established as $Ni_{11}Zr_9$. The unit cell has been observed to be tetragonal with $a_o = 9.90\text{Å}$ and $c_o = 6.62\text{Å}$. Density data indicate that there are two formula weights per unit cell.

A crystal isostructural with the $Ni_{11}Zr_9$ compound has been isolated from a hafnium-nickel alloy. The lattice constants of its unit cell were found to be: $a_o = 9.79\text{Å}$ and $c_o = 6.53\text{Å}$. The space group for these

isostructural compounds has not been completely established, but the possible space groups are; $I\bar{4}$, I4, and I4/m.

The isolation of a single crystal of the compound, Hf_7Ni_{10}, has recently been accomplished. Preliminary X-ray diffraction data indicate the crystal is isostructural with the $Ni_{10}Zr_7$ intermetallic compound.

4.10 Thorium-Tantalum System (W. L. Larsen, D. E. Williams and O.D. McMasters)

The phase diagram of the thorium-tantalum alloy system has been established as being of the simple eutectic type. Homogeneous samples were prepared by repeated arc melting and high temperature vacuum annealing. Melting point determinations of the homogenized samples have established the eutectic isotherm at 1565 $\pm$ 10°C and the eutectic composition at 92.5 w/o thorium. The latter was confirmed by metallography. Melting point data have also been used to establish an approximate liquidus curve.

Both the terminal solubilities are less than three w/o at the eutectic temperature. X-ray diffraction and metallographic data indicate no solubility at room temperature.

Electrical resistance vs temperature data have established the temperature of the transformation in unalloyed thorium as 1365 $\pm$ 15°C. No appreciable change was noted in the transformation temperature with the addition of tantalum. This fact indicates the solubility of tantalum in thorium is very limited near and below 1400°C. Resistance-temperature measurements also verify the eutectic temperature observed in the melting-point determination experiments.

4.11 Uranium-Hafnium System (D. T. Peterson and D. J. Beerntsen)

A report of this investigation entitled "The Uranium-Hafnium Equilibrium System" has been accepted for publication in the Transactions of the American Society for Metals.

Abstract

Hafnium increases the temperature of the alpha-beta uranium transformation on heating from 668°C to 676°C and lowers the beta to gamma transformation to an eutectoid at 733°C and 4.5 a/o hafnium. At elevated temperatures, the body-centered uranium and hafnium are soluble in all proportions and exhibit neither a maximum nor a minimum in the solidus temperatures. Alloys containing 20-65 a/o hafnium, quenched from 1100°C and above, contain a hexagonal delta phase, a = 4.97 Å and c = 3.04 Å, whose X-ray powder pattern is almost identical to that of the delta phase of the uranium-zirconium system. This phase is believed to be a metastable phase, which at equilibrium decomposes to hafnium and uranium. Uranium lowers the alpha-beta transformation in hafnium to a monotectoid at about 1150°C and 55 a/o hafnium. At 1425°C the solubility of uranium in hafnium is between 2.0 and 2.3 a/o.

4.12 Yttrium-Titanium System (O. N. Carlson and D. W. Bare)

The investigation of the yttrium-titanium system was continued during this report period and a terminal report was written and submitted to Transactions of ASM for publication. The paper is entitled, "Phase Equilibria and Properties of Yttrium-Titanium Alloys" by D. W. Bare and O. N. Carlson. A summary of the results of this report is given below.

1. A eutectic reaction occurs at 1330°C and 13 w/o titanium.
2. A peritectic reaction is postulated at 1480°C and 0.2 w/o Ti.
3. The maximum terminal solid solubility at either end of the system is estimated to be less than 1 w/o.
4. Hardness vs composition data measured on alloys at room temperature show a sharp increase in the hardness of Y by the addition of Ti. The hardness of titanium sponge is lowered by the addition of yttrium, probably by oxygen gettering, but titanium crystal bar shows an increase in hardness as a result of yttrium additions.

4.13 Yttrium-Magnesium Alloy Investigation (O. N. Carlson, E. D. Gibson and D. Sauer)

The inital phase of this investigation, a study of the phase relationship between yttrium and magnesium, has been completed and a paper written on this work. The paper entitled "The Yttrium-Magnesium Alloy System" by E. D. Gibson and O. N. Carlson, has been accepted for publication and will appear in the Transactions of the ASM, Vol. 52, 1960. The proposed phase diagram for this system has the following salient features:

1. A eutectic reaction at 74 w/o Mg and 567°C.
2. Maximum primary solid solubility of yttrium in magnesium is 9 w/o Y at the eutectic temperature.
3. There are three intermediate phases designated as γ (Y-Mg) at 21.5 w/o Mg, δ (Y-Mg) at 41 w/o Mg and ε (Y-Mg) at 60 w/o Mg. These are peritectic compounds that decompose at 935°C, 780°C and 605°C, respectively. The phase at 21.5 w/o Mg was identified as YMg from X-ray data.

4. A eutectoid reaction occurs at 775°C and 11 w/o Mg. The reaction is associated with an allotropic transformation in yttrium at high temperatures.

The extensive solid solubility region at the magnesium end of the system suggests the possibility of solid solution strengthening or age-hardening of magnesium by alloying with yttrium. A series of experiments were run on cast alloys containing 1, 2, 3, 4, 5, 6, 7, and 8 w/o yttrium to determine whether the alloys exhibit age-hardening properties. The alloys were solution treated and then heated for five hours at each of the following temperatures: 100, 200, 400, 500 and 600°C. No significant hardening was observed on any of the alloys as a result of the above treatment (see data in Table XXVII). A series was then held for 50 hours at 400°C but no increase in hardness or change in microstructure was observed. It was concluded from these experiments that these alloys do not exhibit age-hardening characteristics. There is, however, appreciable solid solution hardening as indicated by the increase in hardness with increased yttrium content.

Tensile specimens are being prepared from the above alloys for testing at room and elevated temperatures.

Table XXVII

R_H Hardnesses of Mg-Y Alloys with Various Compositions and Heat Treatments

Heat Treatment	w/o Y 1	2	3	4	5	6	7	8
As solution treated	51	61	73	78	82	85	88	92
Annealed at 100	51	61	73	78	82	85	88	92
" " 200	51	62	74	82	83	88	92	94
" " 400	50	58	73	82	84	89	92	96
" " 500	51	60	71	80	81	88	92	96
" " 600	51	61	67	82	83	89	91	95

4.14 Aluminum-Niobium Alloys (H. A. Wilhelm and T. G. Ellis)

The basic process used to prepare Nb-Al alloys was the alumino-thermic reaction of Nb_2O_5. Essentially, this reaction proceeds according to the following equation:

$$3Nb_2O_5 + 10Al \rightleftharpoons 6Nb + 5Al_2O_3$$

Excess Al was added to the charge in the proportion necessary to give the designated alloy composition.

The reaction was carried out in a steel bomb lined with jolt-packed, electrically-fused dolomitic oxide. After carefully filling the reaction chamber with a thoroughly mixed charge, the bomb was sealed and placed in a gas-fired furnace preheated to 600°C. The furnace temperature was

then raised until the reduction within the bomb took place. An indication that the reduction had taken place was given by a sharp increase in the bomb casing temperature, as measured by a thermocouple placed in a well that was attached to the casing.

Results of the direct preparation of Al-Nb alloys by reduction of Nb_2O_5 with Al are given in Table XXVIII.

The maximum amount of Al which could be satisfactorily alloyed with Nb during the alumino-thermic reduction on a small scale, was found to be 70 nominal w/o Al. Attempts to make alloys of higher Al weight percentages resulted in charges which fired but gave little or no massive metal. Therefore, the limit for the size of charge used (1 mole Nb_2O_5 in a 2 1/2" diam. bomb) appears to be 70 w/o to obtain any massive metal at all and 60 w/o to achieve good slag to metal separation.

One major problem in preparing Nb-Al alloys by this method is the difficulty in obtaining segregation of the metal and slag phases; that is, floating all the slag above the compact metal product. The reason for this appears to be associated with a decrease in the maximum temperature of the products after reaction, due to the heat requirements of the large excess of Al added for alloying purposes. Three approaches were made to solve this problem.

Calcium metal was added to the charge in proportions necessary to create a slag of the composition $5CaO \cdot 3Al_2O_3$. The slag segregation from alloys of 65 w/o and 75 w/o Al was very good. However, the metal was porous.

Potassium chlorate ($KClO_3$) was added as a thermal booster to the original Al and a Nb_2O_5 charge was designed to make a 90 w/o alloy. Proportions of $KClO_3$ were added to give 67 and 100 Kcal of heat according to the reaction,

$$KClO_3 + 2Al \rightleftharpoons KCl + Al_2O_3$$

Neither reduction resulted in a metal product. It appeared that more $KClO_3$ should be added to the charge. However, KCl exhibits a high vapor pressure at the temperatures involved in the reduction. This pressure may approach the safe limit of the apparatus. Consequently, the full potentialities of $KClO_3$ as a thermal booster have not yet been thoroughly tested.

A third method of enhancing slag-metal segregation along with producing a more desirable shape of bomb product was the direct casting of rods during bomb reduction of Al-Nb alloys.

A liner of electrically fused dolomitic oxide was jolt-packed in a 2 1/2" diam. steel bomb casing. The mandrel was designed to give a 1/2" diam. x 4" long casting cavity below a 2" diam. x 8" long reactant chamber. An Al foil cone was placed over the casting cavity to prevent the charge from filling it. The bomb was filled with the charge, sealed and fired with the same technique previously mentioned. When the bomb fired, the molten metal melted the Al cone over the casting cavity and allowed the metal to pour into the casting cavity. Results of this technique on several alloys are summarized in Table XXIX.

Table XXVIII

Nominal Alloy Composition w/o Al	Analysed Alloy Composition w/o Al	Alloy Appearance and Slag Segregation
Stio. Charge	3.3	Solid metal biscuit with excellent slag separation and segregation
19	17	Metal and slag separated but not segregated
25	21	Metal and slag separated but not segregated
40	34	Metal in solid biscuit and free of slag
60	56	Metal sponge, fair slag segregation
70	—	Metal droplets in slag powder

Table XXIX

Nominal Alloy Composition w/o Al	Alloy Appearance and Slag Separation
3	Solid metal rod and good slag separation
12	"
16	Solid metal with large slag pockets in the rod
20	"
24	"
50	Spongy metal but good slag separation

4.14.1 Some Properties of Al Rich Al-Nb Alloys

Preliminary studies of the phase relationships of Al rich - Al-Nb alloys began with thermal analysis of alloys containing 3, 5, 10 and 20 w/o Nb.

The alloys were prepared by dissolving Al_3Nb made by bomb reduction in molten aluminum as previously mentioned. The dilution was carried out in Al_2O_3 crucibles using induction heating. Charges of Al and Al_3Nb were heated to 1400°C and held withing $\pm$50°C one half hour. The alloys were then furnace cooled.

Samples of these alloys were sealed in Ta crucibles fitted with thermocouple wells. These samples were placed in a graphite block along with a Ni neutral body and thermally analysed by a differential thermocouple technique. The entire apparatus was placed in an inert He atmosphere and cycled between 500°C and 750°C.

Thermal arrests were noted at 663 -668°C and 616 -621°C.

The samples were thermally analysed in the same apparatus using a 99.99+ Al neutral body sealed in a Ta crucible. The higher arrest was found to be at 658 -659°C. No change was noted in the lower thermal arrest.

No reasonable explanation for the difference in the higher thermal arrest can be given at this time.

4.14.2 Tensile Properties of Some Aluminum Rich Aluminum-Niobium Alloys

Samples of Nb-Al wire of compositions from 0.01 to 0.4 w/o Nb were prepared by diluting a 5.86 w/o Nb master alloy with pure Al. The proper

proportions of Al and master alloy were rocked for eight hours at 800°C in graphite crucibles under a helium atmosphere. After cooling, the samples were cut into 1/4 inch square cross-section rods and swaged to wires 0.047 inches in diameter.

A brief exploratory study of the tensile properties of these alloys was made. All of the specimens were in the cold worked condition including a 99.99+ Al specimen which was prepared in the same manner as the Al-Nb alloys. The wires were tested using a Tinium-Olsen Tensile Tester and a 60 lb. load. These preliminary results indicate that a few hundredths of a percent niobium increases the tensile strength of aluminum markedly.

4.15 The Solubility of Thorium in Vanadium (W. L. Larsen, D. E. Williams and F. E. Palmer)

The metallographic investigation of intermediate and vanadium-rich alloys indicates that the solubility of thorium in vanadium is less than 1 w/o at the eutectic temperature, 1415°C. Electrical resistance vs temperature measurements conducted on the vanadium-rich alloys tend to support the conclusions drawn from the metallographic investigation.

Substantial effort has been expended in the construction and repair of high-temperature X-ray diffraction equipment for the more precise determination of the solubility limits.

An electrolytic etchant has been used with reasonable success in the metallographic investigation of the vanadium-rich alloys. The electrolyte is a 1:1 mixture of 49% hydrofluoric acid and concentrated phosphoric acid. Satisfactory results have been obtained with a current density of 150 ma/sq. in. applied for about ten seconds.

4.16 Crystallographic and Phase Relationships of the Zirconium-Cobalt System

4.16.1 Zirconium-Cobalt Alloy Investigation (W. L. Larsen, D. E. Williams and W. H. Pechin)

The investigation of this system was begun early in the period. A tentative phase diagram for the system is presented in Fig. 6. Two intermediate phases have been reported by other investigators. These are a Laves phase, $ZrCo_2$ and a CsCl-type phase, ZrCo. Melting point and metallographic data verify these and also indicate that there is an intermediate phase corresponding to Zr_2Co. There are thought to be two more compounds in the cobalt-rich portion of the diagram. The exact compositions of these are unknown as yet.

Melting point and metallographic data have been used to determine the following eutectic compositions and temperatures: 17 w/o cobalt, 980°C; 26 w/o cobalt, 1080°C; 42.5 w/o cobalt, 1305°C; and 87 w/o cobalt, 1225°C. The nature of the solidus between 56 and 80 w/o cobalt is still uncertain.

The alpha to beta transformation temperature of the 5 and 12.5 w/o cobalt alloys was determined as 826°C by differential thermal analysis.

Alloys containing from 60 to 70 w/o cobalt have not been successfully prepared by arc melting. Alloys in this composition range shatter during cooling from the molten state. Several of these alloys have been prepared by standard powder metallurgical procedure.

4.16.2 Crystallography (J. F. Smith and D. M. Bailey)

X-ray powder data of CoZr employing CuKα radiations indicate a simple cubic lattice with cell edge a_o = 3.20 Å. Comparison of observed and

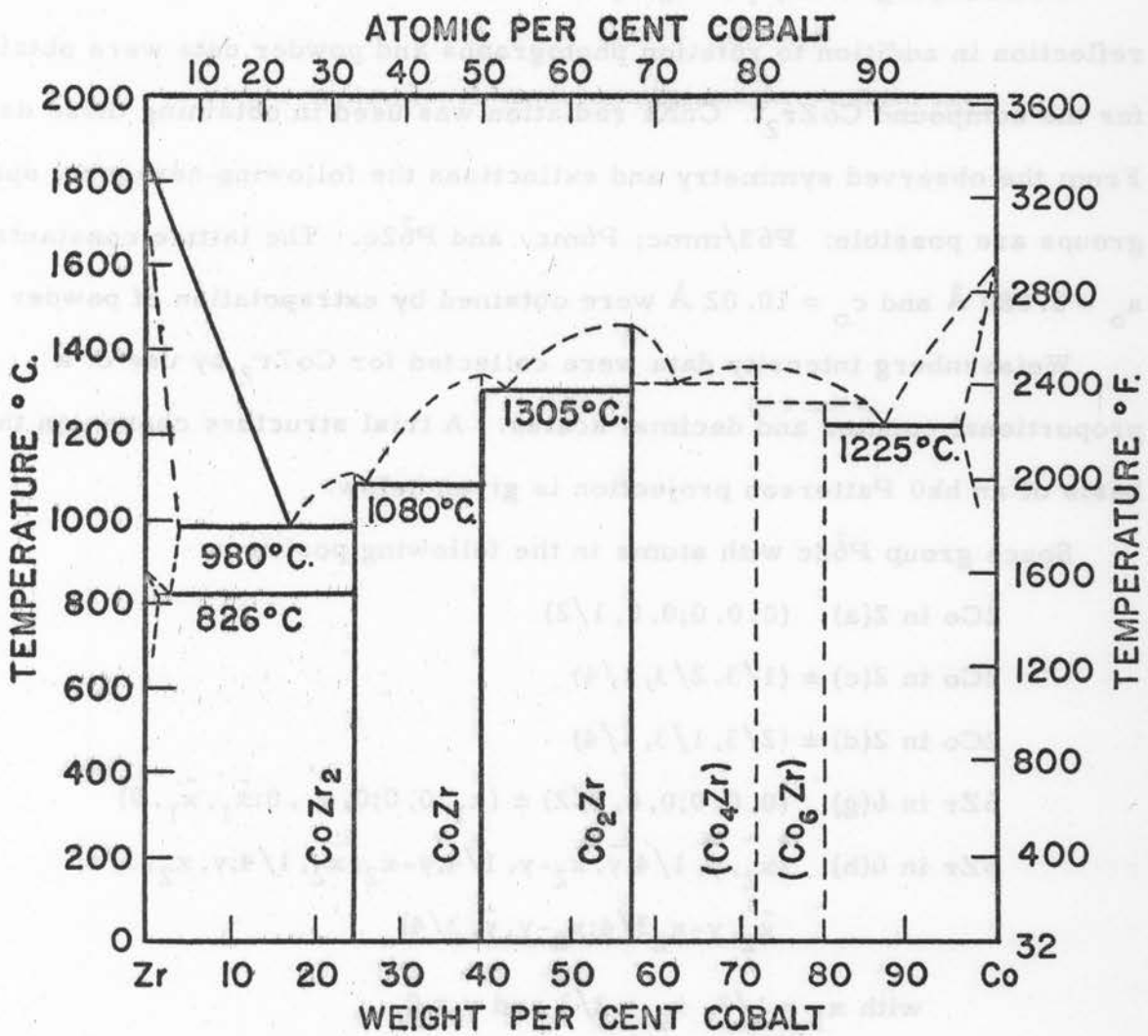

Fig. 6. Tentative phase diagram for cobalt zirconium alloy system.

calculated powder line intensities confirms the CsCl-type structure for CoZr previously reported for this compound by A. E. Dwight of the Argonne National Laboratory.

Weissenberg X-ray photographs of the hk0, hk1, hk2, and hk3 levels of reflection in addition to rotation photographs and powder data were obtained for the compound $CoZr_2$. CuKα radiation was used in obtaining these data. From the observed symmetry and extinctions the following hexagonal space groups are possible: P63/mmc; P6mc, and $P\bar{6}2c$. The lattice constants $a_o = 6.080$ Å and $c_o = 10.02$ Å were obtained by extrapolation of powder data.

Weissenberg intensity data were collected for $CoZr_2$ by use of a proportional counter and decimal scales. A trial structure chosen on the basis of an hk0 Patterson projection is given below.

Space group $P\bar{6}2c$ with atoms in the following positions:

2Co in 2(a) (0, 0, 0;0, 0, 1/2)

2Co in 2(c) ± (1/3, 2/3, 1/4)

2Co in 2(d) ± (2/3, 1/3, 1/4)

6Zr in 6(g) (0, 0, 0;0, 0, 1/2) ± (x_1, 0, 0;0, x_1, 0;$\bar{x}_1$, $\bar{x}_1$, 0)

6Zr in 6(h) (x_2, y, 1/4;$\bar{y}$, x_2-y, 1/4;y-x_2, $\bar{x}_2$, 1/4;y, x_2, 3/4;

$\bar{x}_2$, y-x_2 3/4;x_2-y, $\bar{y}$, 3/4)

with $x_1 = 1/3$, $x_2 = 2/3$ and y = 0.

Initial refinement of this trial structure by means of the LS IIM least squares program for the IBM 650 computer yielded values of $R = \frac{\Sigma \mid F_o \mid - \mid F_c \mid}{\Sigma \mid F_o \mid} = 0.28$ for hk0 data, and R = 0.338 for all layers with parameters $x_1 = 0.34$, $x_2 = 0.71$ and y = 0.

4.17 Barium-Barium Hydride System (D. T. Peterson and M. Indig)

A phase diagram for the Ba-BaH_2 system has been deduced on the basis of thermal analyses, equilibration studies and X-ray diffraction examination. Hydrogen has a considerable solubility in barium. The solubility increases from 8 mol % BaH_2 at 300°C to 67 mol % at 950°C. At 950°C the solid solution decomposes peritectically. The liquidus and solidus temperatures increase smoothly from the melting point of barium at 729°C and extrapolation of the nearly linear liquidus curve indicates a melting point for BaH_2 of 1215°C. A phase transformation of BaH_2 between 500 and 600°C was found. The X-ray diffraction pattern of the high temperature phase was indexed on the basis of a body-centered cubic unit cell. In the Ba-BaH_2 alloys, the temperature of this phase change was raised to 598°C. The results of this investigation are being compiled for publication.

4.18 Aluminum-Yttrium Alloy Studies (H. A. Wilhelm and R. L. Snyder)

Work done on the yttrium-aluminum phase diagram has indicated that the alloy system consists of one congruently-melting compound and two eutectics. This compound corresponds to the formula YAl_2 and crystallizes in a hexagonal crystal system with lattice constants of about 5.245 and 8.375 Å. The melting point of this compound was found to be 1485°C.

The two eutectics were found to be about 9 and 91 w/o yttrium and at temperatures of 644 and 960°C, respectively. In addition to these eutectics, thermal breaks thought to be peritectics were located at temperatures of approximately 980, 1130 and 1080°C.

4.19 Aluminum-Tantalum Alloy Studies (H. A. Wilhelm and D. S. Cowgill)

The purpose of these studies is to determine the phase relationships in the aluminum-tantalum alloy system and to investigate significant properties of the alloys.

The alloys studied to date have been prepared by an aluminothermic reduction method employing tantalum pentoxide and excess aluminum with or without additions of calcium metal to the charge. Small charges employing 1 mol of the oxide are being employed in the exploratory phases of these studies.

Alloys prepared by this method are given an annealing treatment and then studied by metallographic and X-ray diffraction means. Thermal analyses are also being employed to determine the phase relationships. So far compositions of the final alloys are based on calculations from the charge employed in the reduction; chemical analytical results on the alloys have not yet been received.

In addition to the compound Al_3Ta, reported in the literature, there are some evidences of a compound near AlTa and a eutectic near 10 a/o Al. X-ray diffraction data on the Al_3Ta alloy gave constants that check favorably with literature values for that compound. The work is continuing in an effort to obtain a more complete understanding of aluminum-tantalum alloys and their behaviors.

4.20 Uranium-Thorium-Vanadium Ternary Alloys (H. A. Wilhelm and K. M. Wolf)

It has been reported that uranium and thorium alloys at high temperatures are composed of two immiscible liquids over a rather wide range of composition.

The uranium-vanadium and thorium-vanadium binary systems, however, are reported to be of rather simple eutectic type. Major interests in the ternary system include a knowledge of the effect of vanadium additions on the elimination of the liquid immiscibility in the uranium-thorium rich alloys, and the determination of the compositions of low-melting ternary alloys. It is possible that a homogeneous low-melting ternary liquid phase of these metals could be of interest as a fuel material for certain nuclear reactors.

Alloys studied to date have been prepared by co-melting the metals by means of the electric arc. Y_2O_3 and BeO crucibles have been employed in making subsequent melting and thermal studies of the alloys. Major segregation has been observed in some of the low vanadium content alloys on remelting in a resistance heated furnace. Stirring these same alloys by induction during remelting does not permit adequate conditions for good segregation. A ternary eutectic from a one phase liquid alloy appears to be likely in the area of 5 w/o V, 5 w/o Th and 90 w/o U, at a temperature of about 1020°C.

4.21 Thermodynamic Functions for the Magnesium-Copper and Magnesium-Nickel Systems (J. F. Smith and J. L. Christian)

The magnesium vapor pressures over magnesium-copper and magnesium-nickel alloys have been measured for various compositions by the Knudsen effusion method in the temperature range, 400-1100°K. The free energies, enthalpies, and entropies of formation of Mg_2Cu, $MgCu_2$, Mg_2Ni, and $MgNi_2$ were computed from the vapor pressure data and values are listed in the accompanying table.

Table XXX

Free Energy, Enthalpy, and Entropy of Formation of

$MgCu_2$, $MgNi_2$, Mg_2Cu and Mg_2Ni

Compound	Structure	$-\Delta F_{298}$ (Kcal/g atom)	$-\Delta H_{298}$ (Kcal/g atom)	ΔS_{298} (cal/g atom deg)
$MgCu_2$	C 15	2.1 ± 0.4	1.8 ± 0.4	0.9 ± 0.5
$MgNi_2$	C 36	4.3 ± 0.5	4.4 ± 0.5	-0.2 ± 0.5
Mg_2Cu	~C 16	2.3 ± 0.7	1.3 ± 0.6	3.3 ± 1.2
Mg_2Ni	~C 16	4.7 ± 0.7	5.3 ± 0.7	-2.0 ± 0.9

5. Solid State Investigations

5.1 Magnetic Susceptibility of Vanadium Metal (J. F. Smith and J. D. Greiner)

Measurement of the magnetic susceptibility of vanadium metal prepared by the iodide process has yielded a value of $(5.85 \pm 0.02) \times 10^{-6}$ e.m.u./g. No significant difference was observed between metal in the 'as prepared' and swaged conditions. No field dependence, and hence, no indication of ferromagnetic contaminants, was observed.

5.2 Anisotropic Thermal Expansion of Single Crystals of the Hexagonal Elements, Yttrium, Beryllium, and Zinc (J. F. Smith and R. W. Meyerhoff)

Thermal expansion in single crystals of yttrium, beryllium, and zinc has been measured both parallel and perpendicular to the unique axes. The

temperature range for the yttrium and zinc measurements was 4.2-273°K, while for beryllium the range was 77-273°K. The detecting element for dimensional changes was an interferometer using the Hg line at 5460.7 Å. Difficulties associated with reproducibility at low temperature (ISC-835, p. 47) have been overcome. The zinc data are in good agreement with the earlier work of Gruneisen and Goens[5] in that $\alpha_{\perp}$ was found to become negative at 71°K and to reach a minimum at 48°K, while corresponding values obtained by Gruneisen and Goens were 80°K and 45°K. Numerical values for the thermal contractions are shown in Table XXXI and for the linear coefficients of expansion in Table XXXII.

5.3 Measurements of Elastic Constants of Metal Single Crystals

5.3.1 Beryllium (J. F. Smith and C. L. Arbogast)

Measurements of the five independent elastic constants of single crystalline beryllium (as a function of temperature) have been completed. Values extrapolated to 0°K are: $C_{11} = 29.94 \pm 0.06$, $C_{33} = 34.22 \pm 0.12$, $C_{44} = 16.62 \pm 0.05$, $C_{12} = 2.76 \pm 0.08$, $C_{13} = 1.1 \pm 0.5$ in units of 10^{11} dyne/cm^2. The curves representing the temperature dependence are shown in Fig. 7. Voigt averaging and Reuss averaging of the single crystal elastic constants give excellent agreement because of the small magnitude of the non-diagonal elements, C_{12} and C_{13}. The degree of failure of beryllium to satisfy the Cauchy relations, may reasonably be interpreted to indicate an appreciable contribution from non-central force interactions in the metal.

---

5. E. Gruneisen and E. Goens, Z. Phys. 29, 141 (1924).

Table XXXI

Dimensional Contraction, $(-\Delta L/L_{273})\times 10^4$, for Yttrium, Beryllium, and Zinc

T (°K)	Yttrium ⊥C	Yttrium ∥C	Beryllium ⊥C	Beryllium ∥C	Zinc ⊥C	Zinc ∥C
273.2	0.000	0.000	0.000	0.000	0.000	0.000
250	1.042	4.448	2.344	1.692	2.603	14.080
225	2.146	9.190	4.480	3.275	5.302	29.314
200	3.226	13.852	6.236	4.590	7.846	44.615
175	4.275	18.389	7.624	5.611	10.174	59.983
150	5.282	22.733	8.646	6.300	12.241	75.420
125	6.223	26.813	9.310	6.660	13.878	90.924
100	7.054	30.514	9.647	6.807	15.051	106.424
80	7.576	33.076	9.757	6.819	15.499	118.583
70	7.774	34.167			15.520	124.477
60	7.929	35.108			15.415	130.147
50	8.041	35.878			15.242	135.437
40	8.116	36.449			15.056	140.002
30	8.160	36.813			14.899	143.597
20	8.181	36.918			14.801	146.182
4.2	8.190	37.023			14.755	147.812

Table XXXII

Linear Coefficients of Thermal Expansion for Yttrium, Beryllium, and Zinc (per °K x 10^6)

T (°K)	Yttrium $\perp C$	Yttrium $\parallel C$	Beryllium $\perp C$	Beryllium $\parallel C$	Zinc $\perp C$	Zinc $\parallel C$
273.2-270	4.52	19.22	10.64	7.68	11.36	60.60
250-245	4.45	19.08	9.20	6.74	11.00	60.82
225-220	4.36	18.80	7.62	5.70	10.46	61.10
200-195	4.26	18.38	6.14	4.58	9.70	61.36
175-170	4.10	17.72	4.68	3.32	8.68	61.64
150-145	3.90	16.80	3.20	1.94	7.32	61.90
125-120	3.54	15.50	1.86	0.86	5.58	62.14
100-95	2.90	13.60	0.72	0.16	3.16	61.42
85-80	2.30	11.96	0.38	0.00	1.28	60.10
75-70	1.87	10.56			-0.16	58.50
65-60	1.44	9.02			-1.64	54.10
55-50	1.02	7.24			-1.82	51.70
45-40	0.66	5.22			-1.84	44.10
35-30	0.37	3.08			-1.44	33.50
25-20	0.17	1.28			-0.82	23.30
15-10	0.05	0.24			-0.28	11.00
10-5	0.02	0.08			-0.12	4.20

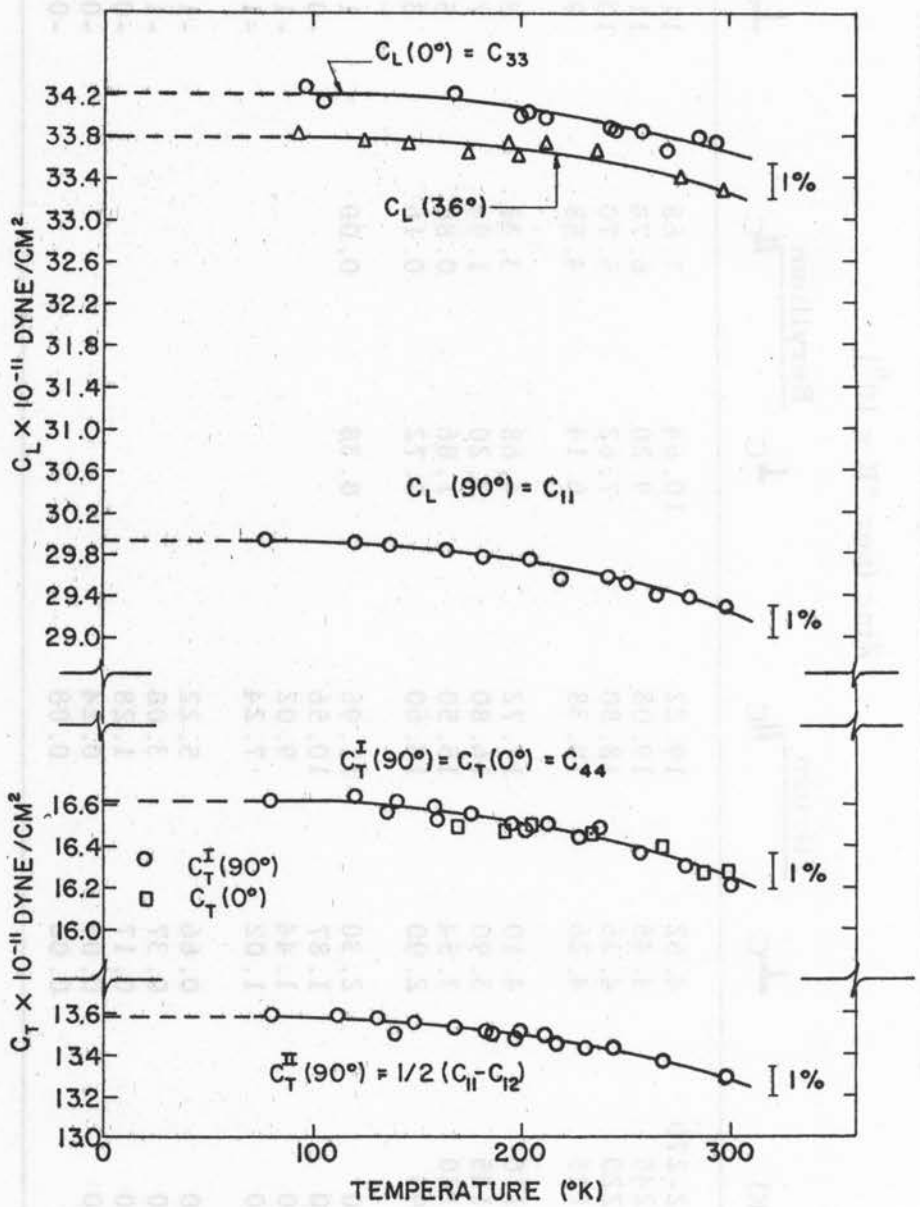

Fig. 7. Adiabatic elastic moduli of beryllium single crystals.

5.3.2 Yttrium (J. F. Smith, J. A. Gjevre and F. H. Spedding)

Two single crystals of yttrium have been prepared so that the five independent elastic constants of hexagonal yttrium may be determined by the pulse-echo method in the temperature range, 4.2-400°K. The constants C_{11} and C_{33} have been determined over the entire temperature range, and it is of interest to note that the curves representing the temperature dependence of these two quantities cross near 390°K. Representative measured values for C_{11} and C_{33} are given in Table XXXIII. Measurements of the other three elastic constants are in progress.

Table XXXIII

Measured Values for C_{11} and C_{33} for Yttrium with Values Corrected for Thermal Expansion (in units of 10^{11} dyne/cm^2)

T(°K)	C_{11}	T(°K)	C_{33}
4.2	8.34	4.2	8.02
78	8.30	78	7.97
115	8.21	120	7.92
203	8.03	202	7.85
298	7.81	298	7.70
357	7.70	332	7.70
411	7.62	396	7.64

5.4 Structure of U_2Zn_{17} (D. T. Peterson and C. L. Vold)

The crystal structure of the intermetallic compound U_2Zn_{17} has been determined. Two modifications, one having hexagonal and one having rhombohedral symmetry, were observed. The structures were similar and differed principally in the stacking of a basic structural layer. A

stacking fault in the hexagonal modification was found. Both structure determinations were refined by a least squares method which produced an R of 0.127 for the rhombohedral structure and of 0.126 for the hexagonal structure when the reflections influenced by the disorder were excluded. The hexagonal structure is related to Th_2Ni_{17} and the rhombohedral structure is related to Th_2Zn_{17}. A report of this investigation is being prepared for publication.

5.5 Deformation Properties of Vanadium at Low Temperatures

The investigation of the low temperature properties of high purity crystal bar vanadium was continued. This included a study of the effects of such variables as strain rate, interstitial impurities, and the substitutional element, (niobium), upon the previously reported brittle-ductile transition in vanadium.

5.5.1 Effect of Strain Rate on Ductility of Vanadium (O. N. Carlson, G. D. Smith and C. V. Owen)

The effect of strain rate and temperature on the ductility of vanadium was studied extensively.[6] Tensile tests were carried out at several temperatures between room and liquid nitrogen temperatures. Indications are that crystal bar vanadium exhibits a change in the slope of the strain rate-ductility surface at the transition temperature. Because of the similarity between these results and those of other investigators on iron,

6. G. D. Smith, "Low Temperature Mechanical Properties of Vanadium", M.S. Thesis, Iowa State University Library, 1958.

it appears that hydrogen embrittlement plays an important role in the mechanism of the ductile-to-brittle transition in vanadium at -100°C and in the return to ductility at still lower temperatures.

The fracture stress is strain rate dependent at all temperatures and shows an increase with increasing strain rate. In general, the effect of increasing temperature is to decrease the fracture stress.

5.5.2 Effects of Interstitials on Ductility of Vanadium (O. N. Carlson, A. Eustice and S. Bradford)

This work consisted primarily of a comprehensive study of the role of hydrogen and oxygen in the embrittlement process.

The tensile test was employed to evaluate the effects of hydrogen on the mechanical properties of iodide vanadium. All specimens were swaged, machined to size, recrystallized at 1120°C, and tensile tested at a strain rate of 0.008 in/in per minute. Table XXXIV illustrates the effect of hydrogen on the ductility and strain-hardening properties of vanadium. The hydrogen content of the vacuum annealed metal was less than 1 ppm. It is noted from the data in the table that the vacuum annealed material does not exhibit a ductility transition in the temperature range studied, whereas the specimens containing 50 ppm hydrogen show a ductile-brittle-ductile fracture sequence generally observed in vanadium metal. A similar sequence is observed in as-prepared crystal bar vanadium which contains approximately 10 ppm hydrogen.

Table XXXIV

Tensile Properties of Vanadium With and Without Hydrogen Addition

Description of Vanadium Specimen	Test Temp	% Uniform Elongation	% Total Elongation	Strain-Hardening Coefficient
Vacuum Annealed	25°C	28.0		- - -
"	-10°	25.0		0.233
"	-50°	21.6		0.211
"	-78.5°	19.5		0.192
"	-120°	18.1		0.142
"	-196°	14.4		0.134
Charged with 50 ppm H_2	25°C	25.5		0.258
"	-35°	14.8		0.249
"	-50°		2.0	*
"	-65°		1.5	*
"	-120°		4.5	0.061
"	-190°	10.7		0.187

* At -50°C and -65°C the specimens necked immediately after plastic deformation began, and the strain-hardening coefficient could not be calculated.

A study was undertaken on the effect of oxygen on the mechanical properties of vanadium and of the deoxidation of vanadium by the addition of several metallic elements. Curves of lattice parameter and hardness vs oxygen content are now being determined by carefully adding weighed amounts of V_2O_5 to the metal in the arc melting step.

5.5.3 Ductility of Vanadium-Niobium Alloys (O. N. Carlson and A. Eustice)

Bend-tests were employed as a method of determining the temperature dependence of the ductility of niobium-vanadium binary alloys. All specimens were recrystallized by annealing in an inert atmosphere. These contained approximately 10 ppm hydrogen and 100 ppm oxygen. The results are given in Table XXXV.

It was believed that hydrogen was responsible for the cracking and brittle fracture which occurred in high-vanadium alloys, but the ductility of the high-niobium alloys was not explained. Analysis by vacuum extraction showed that all alloys contained from 7 to 12 ppm of hydrogen. Bend-test specimens of the 70 Nb-30 V alloy were thermally charged with from 15 to 800 ppm hydrogen. It was found that approximately 20 ppm of hydrogen was necessary to cause embrittlement in this alloy during a bend-test at a ram speed of 0.01 inches per minute.

Tensile data are now being taken on the 30 w/o Nb, 70 w/o Nb and 90 w/o Nb alloys with and without hydrogen additions to confirm the ductility transitions observed in the bend-tests.

Table XXXV

Bend-Test Data on Alloys of V-Nb Binary System Brittle Region

Alloy Composition	Temperature Range	
	High	Low
100 V	- 85°C	-150°C
0.5 Nb - 99.5 V	- 90°	-175°
1.4 Nb - 90.6 V	-105°	---
10 Nb - 90 V	- 95°	-165°
19 Nb - 81 V	- 90°	-180°
30 Nb - 70 V	- 15°	-175°
40 Nb - 60 V	- 22°	-170°
50 Nb - 50 V	- 38°	---
60 Nb - 40 V	- 55°	-150°
64 Nb - 36 V	Ductile above	-196°
70 Nb - 30 V	"	"
80 Nb - 20 V	"	"
90 Nb - 10 V	"	"
100 Nb	"	"

5.6 Anisotropy of Hardness of Yttrium Single Crystals (O. N. Carlson and F. A. Schmidt)

Hardness measurements taken on individual grains of a coarse grained specimen of yttrium metal vary markedly from one grain to another. In an attempt to gain a more complete understanding of this hardness difference, measurements were taken on different faces of a single metal crystal. A single crystal was cut into a parallelepiped approximately 1 cm x 0.75 cm x 0.5 cm, oriented with the c-axis lying in the plane of the larger faces and approximately parallel to the 0.75 cm dimension. Hardness indentations were made by a 1/16 inch diameter ball using the Rockwell "F" scale. Hardness values of 69 were obtained on the largest (front) face, 67 and 72 on the end faces and 86 and 89 on the side faces of the rectangular body. The three lower hardness values were obtained on faces lying at right angles to the basal plane, and gave elliptically distorted indentations with the major axis of the ellipse lying parallel to the basal plane. The holes in the faces lying almost parallel to the basal planes (the two higher hardness values) were round. Since the basal plane is generally the plane of easy slip in a hexagonal metal, deformation in the [001] direction (along the c-axis) occurs with the greatest difficulty. Thus a hardness reading taken down the c-axis encounters the maximum resistance to deformation resulting in a uniform distortion but a smaller area of indentation. Measurements taken on other faces deform readily in the basal plane, which gives a deeper penetration of the indenter, but a non-uniform plastic

deformation in the area of the indentation. This work is described in the paper "Survey of the Mechanical Properties of Yttrium and Yttrium Alloys" by O. N. Carlson, D. W. Bare, E. D. Gibson and F. A. Schmidt, which has been accepted for presentation at the ASTM meeting in San Francisco, in October, 1959. The paper will also be published in one of the technical publications of the Society.

5.7 Growth of Yttrium Single Crystals (O. N. Carlson and E. D. Gibson)

Several large single crystals of yttrium have been grown by solid state methods. By annealing arc-melted pieces of the metal at 1300°C for twenty-four hours, crystals as large as 1" x 5/8" in diameter have been grown. The samples were highly polished before annealing, since this procedure seems to favor larger growth of the grains. The crystals grown to date have been used for ultrasonic determination of elastic constants, electrical resistivity and thermal expansion measurements. A few small crystals were also prepared for the study of the hardness and deformation properties of yttrium.

5.8 Plastic Properties of Thorium (D. T. Peterson)

A previous study of the effect of hydrogen on the ductility of thorium had indicated that the 0.2% offset strength of thorium was reduced by hydrogen. An investigation of the plastic properties of Ames thorium was undertaken to elucidate the effect of hydrogen on these properties. The plastic properties were studied by measuring the stress required to cause flow in a tensile sample at a constant strain rate at room temperature. The flow stress

(stress required to cause further elongation of a tensile sample) at constant strain was found to be quite dependent on the rate of straining. A linear relationship was found between the flow stress and the logarithm of the strain rate from strain rates of 1.2×10^{-3} to 1.4 per minute. The flow stress also was a function of strain. From 4% elongation to 60% elongation, the flow stress at a constant strain rate was proportional to the logarithm of the strain. Thus for Ames thorium at room temperature, the flow stress can be expressed in an equation stress = $K_1 + K_2$ log strain + K_3 log strain rate.

Thorium has a pronounced yield phenomenon in the annealed condition. The stress at the upper and lower yield points increased with strain rate nearly the same as the flow stress for the remainder of the strain range. The yield phenomenon was reduced by the addition of hydrogen and was completely eliminated by 25 ppm hydrogen in slow cooled samples and by 10 ppm in samples quenched from 400°C.

The plastic properties of thorium will be studied at temperatures from -196 to +500°C as a continuation of this investigation.

5.9 Electron Distribution in V_4Al_{23} (J. F. Smith and A. E. Ray)

Three dimensional X-ray diffraction intensity data have been collected from a spherical crystal of V_4Al_{23} by the moving crystal-stationary counter technique. Corrections were made for the effects of absorption, dispersion, extinction, and anisotropic thermal motion of the atoms. The crystal structure was refined by the method of least squares and by difference

syntheses to a reliability index of 0.057. The intensity data were placed on an absolute scale using only those reflections for which $(\sin \theta)/\lambda > 0.29$ Å^{-1}, and which are relatively insensitive to the distribution of the outer electrons. Difference syntheses were then computed for the reflections, $(\sin \theta)/\lambda < 0.29$ Å^{-1}, which are most sensitive to the distribution of the outer electrons. These difference syntheses are a measure of the difference between the equilibrium electron distribution in the crystal and that in the isolated free atoms. The results do not indicate an increased electron concentration in the vanadium d-levels, as proposed by Raynor, but do show indication of directional character in the bonding.

6. Other Investigations

6.1 Diffusion of Hydrogen in Thorium (D. T. Peterson and D. G. Westlake)

The rate of diffusion of hydrogen in thorium was determined by measuring the rate of hydrogen evolution from hydrogen-containing samples under vacuum, and by measuring the axial concentration gradient in cylindrical samples after charging with hydrogen. The two methods were used in different temperature ranges, but gave diffusivity values which fell on the same straight line in a plot of the logarithm of the diffusivity against reciprocal temperature. The diffusivity from 300° to 900°C is given by the equation,

$$D = 2.92 \times 10^{-3} \exp^{-9,750/RT}.$$

The rate evolution of hydrogen was found to be very greatly reduced by surface contamination and great care was taken to prevent this contamination. However, experiments in which a surface layer was influencing the rate could be detected by the abnormal shape of the rate-time curves. The diffusivity was found to increase with increasing hydrogen content above 600°C. No concentration dependence of the diffusivity was found at lower temperatures.

6.2 The Absorption of Hydrogen by Thorium (D. T. Peterson and D. G. Westlake)

The results of this investigation have been accepted for publication in the Journal of Physical Chemistry. An abstract of the paper, "The Rate of Reaction of Hydrogen with Thorium," is given here:

The reaction between thorium and hydrogen, which produced a surface layer of thorium dihydride, was shown to follow the parabolic rate law. At pressures slightly greater than the dissociation pressure of the dihydride, the absorption rate was very dependent on the pressure, but at higher pressures the pressure dependency was less pronounced. Increasing the temperature accentuated the pressure dependency of the absorption rate at the higher pressures. The temperature dependence of the absorption rate satisfied an Arrhenius type equation at temperatures below 550°C when the pressure was held constant at 120 mm. The activation energy for diffusion was found to be about 19.6 Kcal. The absorption rate was the same for annealed thorium of two purity levels and for cold-swaged thorium.

6.3 Vapor Pressure of Calcium over Solutions of Calcium in Molten Calcium Chloride (D. T. Peterson and E. Johnson)

The vapor pressure of calcium over solutions of calcium in molten calcium chloride is being measured by a carrier gas method. The apparatus has been used very successfully to measure the vapor pressure of pure calcium from 800° to 1100°C. The measured vapor pressures agree quite well with the measurements of Smith at lower temperatures, and Hartmann and Schneider at higher temperatures. The vapor pressure of calcium is being measured over a range of calcium concentrations, as the dependence of the vapor pressure on concentration will give considerable information on the nature of the solutions of calcium in molten halides.

6.4 The Effect of ThO_2 on Thorium-Hydrogen Equilibrium (D. T. Peterson, D. G. Westlake and J. Rexer)

A report of this investigation has been accepted for publication in the Journal of Physical Chemistry, in September, 1959, under the title "The Effect of Thorium Oxide on Thorium-Hydrogen Equilibrium."

Abstract

The increase in hydrogen dissociation pressure with hydrogen content, at constant temperature, in the two phase thorium-thorium hydride region, has been shown to be related to the dissolution of thorium oxide in thorium hydride. Thorium oxide does not change the equilibrium pressure over the solid solution of hydrogen in thorium, nor does it change the hydrogen to free metal ratio in thorium hydride. Thorium hydride with 4.0% ThO_2 in

solution was found to be face-centered-cubic rather than tetragonal. The volume per formula weight was nearly the same for both modifications so that this change probably does not indicate a significant change in the type of bonding.

6.5 Phase Relationships and Thermodynamics of the Th-ThH_2-ThC System (D. T. Peterson and J. Rexer)

The Th-ThH_2-ThC system has been studied by means of pressure composition isotherms and X-ray diffraction. Two ternary compounds, $ThH_2 \cdot ThC$ and $2ThH_2 \cdot ThC$ were found and characterized. Both compounds were brittle, metallic in appearance and had lower hydrogen equilibrium pressures than ThH_2 at the same temperature. The hydrogen equilibrium pressure for $ThH_2 \cdot ThC$ in equilibrium with thorium metal and ThC is given by $\log P_{mm\ Hg} = \frac{-10,580}{T} + 10.20$. The structure of this compound has thorium atoms in a hexagonal closed packed arrangement with apparent unit cell dimensions $a_o = 3.816$ Å and $c_o = 6.302$ Å. The enthalpy of formation of this compound from thorium, ThC and hydrogen gas is -48.4 Kcal per mole of H_2. The hydrogen equilibrium pressure for $2ThH_2 \cdot ThC$ is given by $\log P_{mm\ Hg} = \frac{-8,365}{T} + 9.836$. The structure seems to be based on a monoclinic unit cell with $a_o = 6.50$ Å, $b_o = 3.80$ Å, $c_o = 10.91$ Å and $\beta = 119°$. The enthalpy of formation of this compound from thorium, $ThH_2 \cdot ThC$ and hydrogen gas is -38.3 Kcal per mole of hydrogen.

The activity of hydrogen in solid solution in thorium did not seem to be changed by variation in the carbon content. Consequently, the concentration of hydrogen in thorium in equilibrium with the ternary compounds was much lower than that in equilibrium with ThH_2.

The investigation of the thorium ternary system has been completed and a study of the zirconium, titanium and hafnium systems has been started.

6.6 Reduction of Vanadium Oxytrichloride with Hydrogen (R. E. McCarley and J. W. Roddy)

The reaction of $VOCl_3$ with hydrogen was performed at temperatures from 500° to 850°C. In these experiments, electrolytic grade hydrogen was passed through a "Deoxo" catalyst unit to remove oxygen, dried by passage through concentrated sulfuric acid followed by a liquid nitrogen trap, and then bubbled through $VOCl_3$. The partial pressure of $VOCl_3$ in the gaseous mixture was regulated by control of the temperature of the liquid between 25 and 100°C. Subsequently, the mixture was passed through a glass tube at 400° for preheating, thence through a second tube, which was maintained at the desired reaction temperature. All gaseous products were then conducted to the atmosphere through a concentrated sulfuric acid scrubber which served to remove vanadium compounds and to protect the system from the atmosphere.

Results of several of the reactions are tabulated in Table XXXVI. Evidence of reaction was not found below ca 550°C. Within the rather narrow temperature range of 600 to 650° vanadium (III) oxychloride was

Table XXXVI

Results of the Reaction of $VOCl_3$ with Hydrogen

Temperature of $VOCl_3$ bath (°C)	Reaction Temperature (°C)	Time of Reaction (hours)	Amount of Materials Produced		
			V_2O_3	VOCl	VCl_2
~25	550	9	nil	trace	nil
~25	600	5	nil	major	nil
80	610	2.75	nil	major	nil
75	635	6.5	nil	major	nil
~25	650	4	trace	major	trace
60	690	5.5	moderate	moderate	moderate
80	700	2.5	moderate	moderate	moderate
~25	755	5	major		trace
~25	850	5	major	nil	nil

the sole product. Above 650°, but below 750°, a mixture of the products VOCl, V_2O_3, and VCl_2 resulted, while evidence indicated that above 750° vanadium metal and V_2O_3 were the products. Identification of the products was based on both analytical data and X-ray powder diffraction patterns for the mixtures.

In order to understand the course of the reaction as a function of temperature, additional work was performed on the high temperature stability of vanadium (III) oxychloride, VOCl. Thus, several grams of VOCl contained

in a 15 mm Vycor tube were decomposed under 1×10^{-3} mm pressure by gradually raising the temperature. At ca 600-650°C decomposition occurred with formation of V_2O_3, VCl_3, VCl_4 and VCl_2. The VCl_3 sublimed out of the hot zone and condensed on the walls of the reaction vessel, while the VCl_4 distilled out of the vessel and was condensed as a brown solid in a trap at -190°. The solid residue consisted of black, powdery V_2O_3 and large green, lamellar crystals of VCl_2. At 800-850° sublimation of the VCl_2 became evident but was very slow. Owing to the instability of VCl_3 at 650°, the following reactions are thought to be those of importance in the decomposition of VOCl.

$$(1)\quad 3VOCl = V_2O_3 + VCl_3$$

$$(2)\quad 2VCl_3 = VCl_2 + VCl_4$$

$$(3)\quad 6VOCl = 2V_2O_3 + VCl_2 + VCl_4$$

These reactions, therefore, are largely responsible for the mixtures that result when $VOCl_3$ is reduced with hydrogen at temperatures above 650°. Since VCl_4 has not been observed as a product of the hydrogen reduction, reaction (4) must occur also.

$$(4)\quad VCl_4 + H_2 = VCl_2 + 2HCl$$

Above 750° the only products are V_2O_3 and vanadium metal as a result of further reaction of VCl_2 with hydrogen.

$$(5)\quad VCl_2 + H_2 = V + 2HCl$$

Thus, only within the rather limited temperature range of 600-650° is the single, pure compound VOCl formed in the reaction of hydrogen with $VOCl_3$.

Lattice constants for pure VOCl and VCl_2 have been determined from the X-ray powder patterns for these substances. We have found the VOCl to have orthorhombic structure, a = 3.78 Å, b = 3.30 Å and c = 7.97 Å; it is isotypic with FeOCl. Vanadium (II) chloride was determined to be in the rhombohedral crystal system with lattice constants a = 6.20 Å and α = 33.8°. The structure may also be represented by a pseudo hexagonal cell with a' = 3.60 Å and c = 17.50 Å.

6.7 Mechanical Properties of Yttrium and Yttrium Alloys (O. N. Carlson, E. D. Gibson, D. W. Bare and F. A. Schmidt)

A survey of the mechanical properties of yttrium and the effects of fifteen different interstitial and substitutional solutes and dispersed phases on its tensile strength, ductility and hardness are described in a paper entitled "Survey of the Mechanical Properties of Yttrium and Yttrium Alloys" by O. N. Carlson, D. W. Bare, E. D. Gibson and F. A. Schmidt. This paper is scheduled for presentation at the Pacific Area National Meeting of the American Society for Testing Materials in October, 1959, and will be published in a special technical publication of the Society.

6.8 The Chemistry of Niobium(III) and (IV) (R. E. McCarley and O. C. Martin)

Very little work pertaining to the solution chemistry of niobium in its lower oxidation states has appeared in the literature. There is good evidence for niobium(III) and (IV) in aqueous solutions, but these states, in the absence of complexing agents, are unstable and are oxidized by

the solvent to niobium(V). This work was undertaken in an effort to stabilize the lower oxidation states by either coordination or working in solutions of non-aqueous solvents.

Since acetylacetone forms stable complexes with a wide spectrum of metals, initial attempts at stabilization by coordination were made with the use of this reagent. Niobium(III) iodide was used initially as a starting material in order to eliminate the necessity of a reduction. However, the conditions that were required for the reaction, either in the presence or absence of solvent, apparently resulted in decomposition of the products. This has been attributed to the insolubility of NbI_3 in most solvents and to its rather unreactive nature. Subsequent reactions were performed with $NbBr_5$ as starting material. Products of these reactions have not as yet been characterized, but work in this direction is in progress.

In the course of this investigation a rather interesting reaction between $NbBr_5$ and pyridine has been observed. When $NbBr_5$ was dissolved in anhydrous pyridine at room temperature the solution initially exhibited the characteristic maroon color of the $NbBr_5$. After a short time a green precipitate appeared and continued to form until after approximately 3 to 4 hours the solution was colorless and all of the niobium had precipitated. Evidence obtained at this time indicates that the niobium is in either the +3 or +4 oxidation state in the green compound. Pyridinium bromide and bromopyridine were apparently the other products of the reaction. Work now in progress is designed to determine the structure of this compound and to elucidate the oxidation state of the niobium.

6.9 Distribution of Silver and Copper Between Liquid Lead and Zinc

(D. T. Peterson and R. Kontrimas)

The distribution of silver between liquid lead and zinc has been studied at several temperatures. The distribution coefficient was measured by using Ag^{110} as a tracer and counting aliquots of samples from each liquid phase. The distribution coefficient did not change with concentration over a concentration range from 5×10^{-5} to 6×10^{-2} atom fraction of silver in zinc. The values at three temperatures are given in Table XXXVII where K_d is the ratio of the atom fraction silver in zinc to the atom fraction in lead. The enthalpy of transfer was -10.9 Kcal per mole. The study of the distribution of silver has been concluded, and that of copper has been started. A colorometric method of determining copper has been modified for use in this investigation.

Table XXXVII
Distribution Coefficient of Silver between
Liquid Lead and Zinc

Temperature	K_d
438	55.7 ± 2.1
508	27.5 ± 0.5
548	20.1 ± 1.1

6.10 Solubility of Thorium Dihydride in Thorium Metal (D. T. Peterson and D. G. Westlake)

The results of this study have been published in the Transactions of the AIME, Vol. 215, 444 (1959). The title of the paper is "Solubility of Thorium Dihydride in Thorium Metal".

Abstract

The saturation solubility of thorium dihydride in thorium was studied by saturation of samples and subsequent analysis. The solubility increased from about 1 a/o at 300°C to above 20 a/o at 800°C. Over this temperature range the log of the solubility was a linear function of the reciprocal absolute temperature for thorium of good purity. The heat of solution of thorium dihydride was found to be 7.9 Kcal per atom of hydrogen in crystal bar thorium and 6.6 Kcal per atom of hydrogen in Ames thorium.

6.11 Rare Earth Metallurgy

See Chemistry Semi-Annual Summary Research Report, Ames Laboratory, ISC-1116 (1958) and IS-15 (1959).

APPENDIX I: LIST OF REPORTS FROM THE AMES LABORATORY, JULY-DECEMBER 1958

1. Reports for Cooperating Laboratories

ISC-867 Riley Schaeffer and Hampton Smith. Isotopic Equilibria of Nitrosyl Chloride.

ISC-907 R. D. Redin. Thermomagnetic and Galvanomagnetic Effects.

ISC-941 Robert E. Eberts and F. H. Spedding. Relative Apparent Molal Heat Contents of Some Rare-Earth Chlorides and Nitrates in Aqueous Solutions.

ISC-943 Marlowe Iverson and F. R. Duke. Complex Metal Halides in Fused Alkali Nitrates.

ISC-944 Richard Fleming and F. R. Duke. Transport Numbers and Ion Mobilities in the Fused Salt KCl-$PbCl_2$.

ISC-945 William J. Lane and J. S. Fritz. Metal-Indicator Systems in (Ethylenedinitrilo)tetraacetic Acid Titrations.

ISC-946 Wilfred G. Borduin and G. S. Hammond. Substituent Effects of the Stability of Metal Chelates.

ISC-947 John J. Barghusen and M. Smutz. Processing of Monazite Sands.

ISC-975 Ames Laboratory Staff. Physics. Semi-Annual Summary Research Report. July-December, 1957.

ISC-976 Ames Laboratory Staff. Chemistry. Semi-Annual Summary Research Report. July-December, 1957.

ISC-977 Ames Laboratory Staff. Metallurgy. Semi-Annual Summary Research Report. July-December, 1957.

ISC-978 Ames Laboratory Staff. Engineering. Semi-Annual Summary Research Report. July-December, 1957.

ISC-979 P. Chiotti. Metallurgical Development for Hanford Program. Semi-Annual Report. July-December, 1957.

ISC-1030 R. G. Barnes. Bibliography of Titles of Articles in the Field of Nuclear Quadrupole Resonance Spectroscopy of Solids.

ISC-1037 Benny A. Loomis and O. N. Carlson. Brittle-Ductile Transition in Vanadium.

ISC-1045 Wilfred G. Borduin and G. S. Hammond. Further Relationships in the Grunwald Treatment of Acid-Base Equilibria in Hydroxylic Solutions.

ISC-1047 R. M. Stanton, P. F. Woerner, C. L. Vold, J. A. Kingston, and J. F. Smith. Tabulation, Bibliography, and Structure of Binary Intermetallic Compounds. IV. Compounds of Zinc, Cadmium and Mercury.

ISC-1048 Ames Laboratory Staff. Physics. Semi-Annual Summary Research Report. January-June, 1958.

ISC-1051 Ames Laboratory Staff. Engineering. Semi-Annual Summary Research Report. January-June, 1958.

ISC-1056 Richard T. Oliver and James S. Fritz. Ion-Exchange Separation of Metals by a Single Pass Method.

ISC-1059 Robert L. Skaggs and D. T. Peterson. Entrainment of Non-Volatile Solids in Sublimation at Reduced Pressure.

ISC-1074 Peter H. Vossos and R. E. Rundle. Crystal Structure and Magnetic Properties of $LiCuCl_3 \cdot 2H_2O$.

2. Publications

Amma, E. L. and R. E. Rundle
Electron Deficient Compounds. VIII. The Crystal and Molecular Structure of Trimethylindium. J. Am. Chem. Soc. 80, 4141-4145 (1958).

Anderson, Gerald S. and Sam Legvold
Conduction Electron-Magnetic Ion Interaction in Rare Earths. Phys. Rev. Letters 1 1-2 (1958).

Anderson, G. S., S. Legvold and F. H. Spedding
Hall Effect in Lu, Yb, Tm, and Sm. Phys. Rev. 111, 1257-1258 (1958).

Arajs, Sigurds and Sam Legvold
Electroconvectional Heat Transfer in Gases. J. Chem. Phys. 29, 531-536 (1958).

Arajs, Sigurds and Sam Legvold
Free Convectional Heat Transfer from a Single Horizontal Wire. J. Chem. Phys. 29, 697-699 (1958).

Banks, Charles V., Clara I. Adams and John Richard
Solubility of vic-Dioximes in Urea Solutions. Anal. Chim. Acta 19, 531-539 (1958).

Banks, Charles V. and Dennis W. Barnum
Intermolecular Metal-Metal Bonds and Absorption Spectra of Some Nickel(II) and Palladium(II) Complexes of vic-Dioximes. J. Am. Chem. Soc. 80, 4767-4772 (1958).

Banks, Charles V., Keith E. Burke and Jerome W. O'Laughlin
The Determination of Fluorine in Rare Earth Fluorides by High Temperature Hydrolysis. Anal. Chim. Acta 19, 239-243 (1958).

Banks, Charles V., J. P. LaPlante and John J. Richard
Preparation of 4-Carboxy-1,2-Cyclohexanedionedioxime. J. Org. Chem. 23, 1210-1211 (1958).

Banks, Charles V., James A. Thompson and Jerome W. O'Laughlin
Separation and Determination of Small Amounts of Rare Earths in Uranium. Anal. Chem. 30, 1792-1795 (1958).

Barnes, R. G. and R. D. Engardt
Unusual Temperature Dependence of Bromine Quadrupole Resonances in $TiBr_4$. J. Chem. Phys. 29, 248-249 (1958).

Barnes, R. G. and R. A. Hultsch
Indirect Nuclear Spin-Spin Interactions in Pure Quadrupole Resonance Spectra. Phys. Rev. Letters 1, 1-2 (1958).

Barghusen, John, Jr. and Morton Smutz
Processing of Monazite Sands. Indus. Eng. Chem. 50, 1754-1755 (1958).

Corbett, John D.
Bismuth(I) Chloride. J. Am. Chem. Soc. 80, 4757-4760 (1958).

Corbett, John D.
Evidence on the Nature of Bismuth(I) Chloride Formed by Solution of Bismuth in Bismuth(III) Chloride. J. Phys. Chem. 62, 1149 (1958).

Dahl, June L. and Frederick R. Duke
Surface Tensions of the $AgNO_3$-$NaNO_3$ and $AgNO_3$-KNO_3 Systems. J. Phys. Chem. 62, 1142-1143 (1958).

Duke, Frederick R. and James P. Cook
A Non-Visual Method for Transport Numbers in Pure Fused Salts. II. Iowa State Coll. J. Sci. 35, 81-83 (1958).

Duke, F. R. and R. A. Fleming
The Equivalent Conductivities of $AgNO_3$-KNO_3 Mixtures. J. Electrochem. Soc. 105, 251 (1958).

Duke, Frederick R. and Marlowe L. Iverson
Acid-Base Reactions in Fused Salts. I. The Dichromate-Nitrate Reaction. J. Am. Chem. Soc. 80, 5061-5063 (1958).

Duke, F. R. and Boone Owens
The Mobilities of the Ions in Fused KNO_3-$AgNO_3$ Mixtures. J. Electrochem. Soc. 105, 476-477 (1958).

Duke, Frederick R. and Boone Owens
Transport Numbers of the Pure Fused Salts, $LiNO_3$, $NaNO_3$, KNO_3, and $AgNO_3$. J. Electrochem. Soc. 105, 548-549 (1958).

Flesch, Gerald D. and Harry J. Svec
New Preparations for Chromyl Fluoride and Chromyl Chloride. J. Am. Chem. Soc. 80, 3189-3191 (1958).

Fritz, James S., Marlene J. Richard and Shirley K. Karraker
Potentiometric Titrations with (Ethylenedinitrilo)tetraacetate. Anal. Chem. 30, 1347-1350 (1958).

Fritz, James S., Marlene Johnson Richard and William J. Lane
Spectrophotometric Determination of Rare Earths. Anal. Chem. 30, 1776-1779 (1958).

Fritz, James S. and Gerald R. Umbreit
Ion Exchange Separation of Metal Ions. Anal. Chim. Acta 19, 509-516 (1958).

Hammer, C. L. and R. H. Good, Jr.
Quantization Process for Massless Particles. Phys. Rev. 111, 342-345 (1958).

Herman, R. and C. A. Swenson
The Temperature Dependence of the Phase Transition in Cerium. J. Chem. Phys. 29, 398-400 (1958).

Jennings, L. D. and C. A. Swenson
The Effects of Pressure on the Superconducting Transition Temperatures of Sn, In, Ta, Tl and Hg. Phys. Rev. 112, 31-43 (1958).

Junk, Gregor and Harry J. Svec
The Absolute Abundance of the Nitrogen Isotopes in the Atmosphere and Compressed Gas from Various Sources. Geochim. Acta 14, 234-243 (1958).

Kniseley, Richard N., Velmer A. Fassel, Beverly B. Quinney, Carl Tremmel, William A. Gordon and William J. Hayles
Determination of Rare Earth Impurities Commonly Associated with Purified Samarium, Gadolinium, Terbium and Yttrium. Spectrochim. Acta 12, 332-337 (1958).

Laslett, L. Jackson
The Field of a Linear Electrostatic Multipole. Am. J. Phys. 26, 402-403 (1958).

McCarley, Robert E., Don S. Martin, Jr. and Lee T. Cox
Solid State and Solution Exchange of Platinum Between $[Pt(en)Br_2]$ and $[Pt(en)Br_4]$. J. Inorg. Nucl. Chem. 7, 113-118 (1958).

McMullan, Richard K. and John D. Corbett
The Lower Oxidation States of Gallium. III. The Constitution of Ga_2Cl_4 and Its Analogy with $Ga(AlCl_4)$. J. Am. Chem. Soc. 80, 4761-4764 (1958).

Smith, Harold G. and R. E. Rundle
The Silver Perchlorate-Benzene Complex, $C_6H_6 \cdot AgClO_4$, Crystal Structure and Charge Transfer Energy. J. Am. Chem. Soc. 80, 5075-5080 (1958).

Smith, J. F. and J. R. Ogren
Electrical Properties and Thermal Expansion of the Laves Phases, $CaMg_2$ and $MgCu_2$. J. Appl. Phys. 29, 1523-1525 (1958).

Spedding, F. H., K. Gschneidner, Jr. and A. H. Daane
The Crystal Structures of Some of the Rare Earth Carbides. J. Am. Chem. Soc. 80, 4499-4503 (1958).

Spedding, F. H., J. E. Powell, A. H. Daane, M. A. Hiller and W. H. Adams
Methods for Preparing Pure Scandium Oxide. J. Electrochem. Soc. 105, 683-686 (1958).

Svec, H. J., A. A. Read, D. W. Hilker
A Proportioning Furnace Temperature Controller. Iowa State Coll. J. Sci. 33, 139-144 (1958).

Swenson, C. A.
The Phase Transition in Solid Mercury. Phys. Rev. 111, 82-91 (1958).

Thoburn, W. C.
A Portable Magnetic Field and Gradient Meter. Rev. Sci. Instr. 29, 990-992 (1958).

Thoburn, W. C., S. Legvold and F. H. Spedding
The Magnetic Properties of Terbium Metal. Phys. Rev. 112, 56-58 (1958).

Worden, D. G. and G. C. Danielson
Electrical Resistivity of Thin Films of Potassium at 100°K. Phys. Chem. Solids 6, 89-95 (1958).

APPENDIX II: LIST OF REPORTS FROM THE AMES LABORATORY, JANUARY-JUNE 1959

1. Reports for Cooperating Laboratories

ISC-1029 H. A. Wilhelm and R. E. McCarley. List of High Purity Metals Available from American Producers.

ISC-1038 Charles V. Banks, Nelson J. Fowlkes, Peter A. Beak and Michael J. Maximovich. Annotated Bibliography of Alpha-Benzildioxime.

ISC-1049 Ames Laboratory Staff. Chemistry. Semi-Annual Summary Research Report. January-June, 1958.

ISC-1050 Ames Laboratory Staff. Metallurgy. Semi-Annual Summary Research Report. January-June, 1958.

ISC-1052 Ames Laboratory Staff. Metallurgical Development for Hanford Program: Semi-Annual Report. January-June, 1958.

ISC-1058 Donald R. Saxton and Glenn Murphy. Creep of Uranium.

ISC-1068 M. Smutz, G. Burnet, J. Walker, R. Tischer and E. Olson. Preparation of Low Oxygen Content Yttrium Fluoride.

ISC-1069 R. W. Johnson and E. H. Olson. Separation of Cerium from Other Rare Earths by Ignition of the Nitrates.

ISC-1096 S. Katz and A. F. Voigt. Exchange and Chemical Reactions of Cyclopentadienyl, Cobalt Compounds.

ISC-1118 Ames Laboratory Staff. Engineering. Semi-Annual Summary Research Report. July-December, 1958.

ISC-1136 James R. Melcher and Glenn Murphy. Electromagnetic Field Analogy for Neutron Diffusion Theory.

ISC-1144 Ames Laboratory Staff. Metallurgical Development for Hanford Program Semi-Annual Report. July-December, 1958.

ISC-1155 A. E. Ray, J. A. Kingston and J. F. Smith. Tabulation, Bibliography and Structure of Binary Intermetallic Compounds. V. Compounds of Aluminum and Indium.

2. Publications

Armstrong, P. E., O. N. Carlson and J. F. Smith
The Elastic Constants of Thorium Single Crystals in the Range, 77-400°K. J. Appl. Phys. 30, 36-41 (1959).

Atoji, Masao
Anhydrite Obtained by the Dehydration of Gypsum. J. Chem. Phys. 30, 341-342 (1959).

Atoji, Masao
On the Cubic Spherical Harmonics. J. Math. Phys. 38, 73-74 (1959).

Banks, C. V. and Roger E. Yerick
Chelating Properties of N,N,N',N'-Tetrakis(phosphonomethyl)-1,2-cyclohexanediamine. Anal. Chim. Acta 20, 301-314 (1959).

Barnes, R. G., R. D. Engardt and R. A. Hultsch
Nuclear Magnetic Resonance Determination of Activation Volume for Diffusion in Lithium. Phys. Rev. Letters 2, 202-204 (1959).

Baroch, Charles J., Morton Smutz and Edwin H. Olson
Processing of California Bastnasite Ore. Mining Eng. 214, 315-319 (1959).

Beaudry, B. J. and A. H. Daane
The Antimony-Uranium Alloy System. Trans. AIME 215, 199-203 (1959).

Capellen, Jennings and Harry J. Svec
Correction of the Observed Ratio for Errors Associated with Ion Current Collection and Amplification in Dual Collector Mass Spectrometers. Iowa State Coll. J. Sci. 33, 427-430 (1959).

Dorweiler, V. P. and R. W. Fahien
Mass Transfer at Low Flow Rates in a Packed Column. A.I.Ch.E. Journal 5, 139-144 (1959).

Duke, Frederick R.
Acid-Base Reactions in Oxidation Mechanisms. Anal. Chem. 31, 527-529 (1959).

Duke, Frederick R. and Richard A. Fleming
Transport Numbers and Ionic Mobilities in the System Potassium Chloride-Lead Chloride. J. Electrochem. Soc. 106, 130-133 (1959).

Elleman, Thomas S., John W. Reishus and Don S. Martin, Jr.
Trichloroammineplatinate(II) Ion. Hydrolysis, Isotopic Exchange of Chloride and the Trans-Effect. J. Am. Chem. Soc. 81, 10-18 (1959).

Flesch, Gerald D. and Harry J. Svec
The Mass Spectra of Chromyl Chloride, Chromyl Chlorofluoride and Chromyl Fluoride. J. Am. Chem. Soc. 81, 1787-1790 (1959).

Fritz, James S. and Shirley K. Karraker
Ion Exchange Separations. Chromatographic Separations Based on Ion Charge. Anal. Chem. 31, 921-923 (1959).

Fritz, James S. and Marlene Johnson Richard
Colorimetric Uranium Determination with Arsenazo. Anal. Chim. Acta 20, 164-171 (1959).

Fritz, James S., Stanley S. Yamamura and Evelin Carlston Bradford
Determination of Carbonyl Compounds. Anal. Chem. 31, 260-263 (1959).

Haefling, J. F. and A. H. Daane
The Immiscibility Limits of Uranium with the Rare Earth Metals. Trans. AIME 215, 336-338 (1959).

Hansen, Robert S.
Film and Substrate Flow in Surface Channels. J. Phys. Chem. 63, 637 (1959).

Hansen, Robert S.
The Virial Treatment of the Interaction of Gas Molecules with Solid Surfaces. J. Phys. Chem. 63, 743-744 (1959).

Hansen, Wilford N.
Some Magnetic Properties of the Chromium(III) Halides at 4.2°K. J. Appl. Phys. 30, 304S-305S (1959).

Hansen, Wilford N. and Maurice Griffel
The Paramagnetic Susceptibilities of the Chromium(III) Halides. J. Chem. Phys. 30, 913-916 (1959).

Holloway, J. T. and L. Jackson Laslett
The Radiations from Tb^{156}. Phys. Rev. 113, 1581-1583 (1959).

Johnson, Russell W. and Don S. Martin, Jr.
Kinetics of the Oxidation of Cerium(III) by Concentrated Nitric Acid. J. Inorg. Nucl. Chem. 10, 94-102 (1959).

Knapp, Lester, Roman Schoenherr, John Barghusen and Morton Smutz
A Polyethylene Box-Type Mixer-Settler Extractor. Ind. Eng. Chem. 51, 639-640 (1959).

Kniseley, Richard N., Velmer A. Fassel, Raymond A. Tabeling, B. George Hurd and Beverly B. Quinney
Quantitative Spectrographic Analysis of the Rare Earth Elements. X. Determination of Rare-Earth Impurities Commonly Associated with Purified Thulium, Ytterbium, Lutetium and Scandium. Spectrochim. Acta 13, 300-303 (1959).

Laslett, L. Jackson
A Method of Applying Extremal Methods to Problems of Electrical Resistance. Iowa State Coll. J. Sci. 33, 431-439 (1959).

Powell, J. E. and M. A. Hiller
A Method of Adjusting pH Without Introducing Extraneous Cations or Anions. J. Inorg. Nucl. Chem. 9, 100 (1959).

Powell, J. E. and F. H. Spedding
Basic Principles Involved in the Macro-Separation of Adjacent Rare Earths from Each Other by Means of Ion Exchange. A.I.Ch.E. Journal 55, 101-113 (1959).

Savage, William R., Donald E. Hudson and Frank H. Spedding
A Mass Spectrometric Study of Heats of Sublimation of Dysprosium, Samarium, Thulium and Ytterbium. J. Chem. Phys. 30, 221-227 (1959).

Sawada, S. and G. C. Danielson
Domain Structure of WO_3 Single Crystals. Phys. Rev. 113, 1005-1008 (1959).

Sawada, S. and G. C. Danielson
Electrical Conduction in Crystals and Ceramics of WO_3. Phys. Rev. 113, 803-805 (1959).

Sawada, S. and G. C. Danielson
Optical Indices of Refraction of WO_3. Phys. Rev. 113, 1008-1013 (1959).

Schirber, J. E. and C. A. Swenson
The Superconductivity of Mercury. Phys. Rev. Letters 2, 296-297 (1959).

Schupp, Fritz D., Clifford B. Colvin and Don S. Martin, Jr.
Photonuclear Reactions of Gallium and Arsenic with 70-Mev Bremsstrahlung. Phys. Rev. 113, 1095-1098 (1959).

Smith, J. F. and B. T. Bernstein
Effects of Impurities on the Crystallographic Modifications of Calcium Metal. J. Electrochem. Soc. 106, 448-451 (1959).

Smith, J. F. and R. L. Smythe
Vapor Pressure Measurements Over Calcium, Magnesium and Their Alloys and the Thermodynamics of Formation of $CaMg_2$. Acta Met. 7, 261-267 (1959).

Spedding, F. H., K. Gschneidner, Jr. and A. H. Daane
The Lanthanum-Carbon System. Trans. AIME 215, 192-199 (1959).

Spedding, F. H., A. W. Naumann and R. E. Eberts
Heats of Dilution and Related Thermodynamic Properties of Aqueous Rare-Earth Salt Solutions at 25°C; Integral Heats of Solution of $NdCl_3$. J. Am. Chem. Soc. 81, 23-28 (1959).

Wilhelm, Harley A. and Raymond A. Foos
A Countercurrent Liquid-Liquid Extractor. Ind. Eng. Chem. 51, 633-636 (1959).

Williams, Donald E., Gabriele Wohlauer and R. E. Rundle
Crystal Structures of Nickel and Palladium Dimethylglyoximes. J. Am. Chem. Soc. 81, 755 (1959).

APPENDIX III: LIST OF SHIPMENTS, JULY-DECEMBER 1958

Destination	Item
University of California Los Alamos Scientific Laboratory Los Alamos, New Mexico	6 thulium pellets 20 gm thulium metal 100 gm thulium oxide 20 gm lutetium metal 100 gm lutetium oxide
State University of Iowa Iowa City, Iowa	10 gm lanthanum metal 10 gm cerium metal 10 gm praseodymium metal 10 gm neodymium metal 10 gm samarium metal 10 gm gadolinium metal 50 gm lanthanum oxide 50 gm cerium oxide 50 gm praseodymium oxide 50 gm neodymium oxide 50 gm samarium oxide 50 gm gadolinium oxide 50 gm ytterbium oxide 20 gm terbium oxide 10 gm thulium oxide 10 gm lutetium oxide
U. S. Bureau of Mines Albany, Oregon	150 gm dysprosium metal
Ohio State University Columbus, Ohio	100 mg erbium oxide 100 mg cerium oxide 100 mg praseodymium oxide 100 mg neodymium oxide 100 mg samarium oxide 100 mg europium oxide 100 mg gadolinium oxide 100 mg terbium oxide 100 mg dysprosium oxide 100 mg holmium oxide 100 mg erbium oxide 100 mg thulium oxide 100 mg ytterbium oxide 100 mg lutetium oxide
Midwest Microlab, Inc. Indianapolis, Indiana	1 pkg. organo metallic compound
Brown University Providence, Rhode Island	1 lanthanum cylinder

Dr. Joseph Graca Iowa State College Ames, Iowa	5-200 mg pellets each of yttrium metal lanthanum metal cerium metal neodymium metal gadolinium metal ytterbium metal dysprosium metal
	150 pellets, 100 mg each of yttrium metal cerium metal neodymium metal gadolinium metal dysprosium metal ytterbium metal
Duke University Durham, North Carolina	cylinders of neodymium metal as follows: 6 1" x 2" diam. 6 1/2" x 2" diam. 6 1/4" x 2" diam. 6 1/8" x 2" diam.
Battelle Memorial Institute Columbus, Ohio	50 gm dysprosium metal
Carnegie Institute of Technology Pittsburgh, Pennsylvania	5 gm lanthanum metal
General Electric Research Laboratory Schenectady, New York	200 gm yttrium metal
University of Arizona Tucson, Arizona	20 gm neodymium oxide
Syracuse University Syracuse, New York	491 gm calcium

APPENDIX IV: LIST OF SHIPMENTS, JANUARY-JUNE 1959

Destination	Item
Armour Research Foundation Illinois Institute of Technology Chicago, Illinois	200 gm crystal bar vanadium
Physikalisches Institut der Technischen Muchen, Germany	3 rods cerium metal
Argonne National Laboratory Lemont, Illinois	23 yttrium fluoride samples
Karl S. Vorres State University of Iowa Iowa City, Iowa	300 gm lanthanum metal 300 gm cerium metal 300 gm neodymium metal 300 gm yttrium metal 300 gm praseodymium metal 300 gm gadolinium metal 300 gm samarium metal
Biophysics Research Laboratory Peter Bent Brigham Hospital Boston, Massachusetts	5 gm praseodymium oxide 5 gm neodymium oxide 5 gm samarium oxide 1 gm lanthanum oxide 1 gm cerium oxide 1 gm gadolinium oxide 1 gm yttrium oxide 1 gm dysprosium oxide 1 gm holmium oxide 1 gm erbium oxide 1 gm ytterbium oxide 200 mg ytterbium oxide 200 mg thulium oxide 200 mg lutetium oxide
U. S. Bureau of Mines Boulder City, Nevada	27 gm yttrium metal
University of California Los Alamos Scientific Laboratory Los Alamos, New Mexico	200 gm cerium metal 200 gm lanthanum metal sample of octasodium salt of N,N,N',N'-tetrakis-(phosphonomethyl)-1,2-cyclohexanediamine

Destination	Item
University of Arizona Tucson, Arizona	20 gm Gd_2O_3 20 gm Dy_2O_3 20 gm Ho_2O_3 20 gm Pr_6O_{11} 20 gm Er_2O_3 20 gm Yb_2O_3 20 gm La_2O_3 20 gm Ce_2O_3
	5 gm ytterbium oxide
University of New Mexico Albuquerque, New Mexico	5 gm holmium oxide 5 gm thulium oxide 10 gm erbium oxide
Dr. Torgen Huus Universitetets Institut for Teoretisk Copenhagen, Denmark	1 gm yttrium metal 1 gm lanthanum metal 1 gm cerium metal 1 gm neodymium metal 1 gm praseodymium metal 1 gm gadolinium metal 1 gm lutetium metal 1 gm erbium metal 1 gm ytterbium metal 1 gm samarium metal 1 gm terbium metal 1 gm dysprosium metal 1 gm holmium metal 1 gm thulium metal
	5 gm praseodymium oxide 5 gm neodymium oxide 5 gm samarium oxide
	1 gm lanthanum oxide 1 gm cerium oxide 1 gm gadolinium oxide 1 gm yttrium oxide 1 gm dysprosium oxide 1 gm holmium oxide 1 gm erbium oxide 1 gm ytterbium oxide
	200 mg terbium oxide 200 mg thulium oxide 200 mg lutetium oxide
Atomic Energy Research Establishment Harwell, Berkshire, England	1 gm lutetium metal

Destination	Item
Carnegie Institute of Technology Pittsburgh, Pennsylvania	4 gm cerium metal
Michigan Chemical Corporation St. Louis, Michigan	3 10-gm samples yttrium metal
California Institute of Technology Pasadena, California	1 gm N^{15} salt 2 gm ammonium sulfate
Professor Yngve Ohman Stazione Astrofisica Svedese Isola Di Capri, Italy	2 disks gadolinium metal